Liquid-Phase Thermodynamic Properties for the Binary and Ternary Systems of Propane (1), *n*-Butane (2), and Isobutane (3)

Yohei Kayukawa,*,† Masaya Hasumoto,†,‡ Yuya Kano,† and Koichi Watanabe†

School of Science for Open and Environmental Systems, Graduate School of Science and Technology, Keio University, 3-14-1, Hiyoshi, Kohoku-ku, Yokohama 223-8522, Japan

Experimental thermodynamic property data for hydrocarbon refrigerant mixtures are more important now in order to improve the performance of existing equations of state. In the present paper, liquid-phase *PVTx* data including bubble points for the binary and ternary systems composed of propane (1), *n*-butane (2), and isobutane (3) are reported. More than 1000 measurements were made by employing a newly developed vibrating-tube densimeter system with an uncertainty of 0.1 kg·m^{-3} + 0.024% for density, (3 to 7) mK for temperature, 0.26 kPa + 0.022% for pressure, and 0.1 mol % for composition. The present data contain the first set of experimental *PVTx* data for the ternary system. The measured data are compared with two available thermodynamic mixture models developed by Lemmon and Jacobsen and Miyamoto and Watanabe. A mixture model applied for a modified Tait equation of state is also presented in this paper.

Introduction

The production of refrigeration systems, especially household refrigerators, with hydrocarbon refrigerants is rapidly increasing with nonhalogenated refrigerants. Mathematical models that represent the thermodynamic properties of refrigerants are called equations of state (EoS), and their role as a cycle-performance estimation tool, or standard values of thermodynamic properties, is significant in the R&D activities of HVAC & R engineering. The latest EoS for propane (1), *n*-butane (2), and isobutane (3) formulated by Miyamoto and Watanabe[1−3] are now included in the thermodynamic-property calculation software REFPROP (version 7.0)[4] released by NIST (the National Institute of Standards and Technology, Boulder, Colorado).

To improve the cycle efficiency of refrigeration systems, the use of refrigerant mixtures to realize the Lorentz cycle is of concern. Equations of state for mixtures are now more important to match the increasing demand for accurate thermodynamic-property values of refrigerant mixtures. Such a function is available with REFPROP. It employes the generalized mixing rule for the Helmholtz free energy proposed by Lemmon and Jacobsen[5] and was developed on the basis of experimental data for selected mixtures. However, the reproducibility of the model may sometimes be unknown for unstudied mixture systems, such as hydrocarbon mixtures. Miyamoto and Watanabe[6] have also developed a mixture thermodynamic model for hydrocarbon mixtures composed of propane (1), *n*-butane (2), and isobutane (3). They developed their model on the basis of the available experimental data for the mixtures. We intend to evaluate these two available mixture models by comparing them with new data for hydrocarbon mixtures.

* To whom correspondense should be addressed. Present affiliation: Fluid Properties Section, Material Properties and Metrological Statistics Division, National Metrology Institute of Japan, National Institute of Advanced Industrial Science and Technology, AIST Tsukuba Central 3, Tsukuba 305-8563, Japan. Tel: +81-29-861-6833. Fax: +81-29-850-1464. E-mail: kayukawa-y@aist.go.jp.

† Keio University.

‡ Present affiliation: Builiding Systems Solution Department, Building Systems Development Center, Matsushita Electric Works, Ltd., 1048, Kadoma, Osaka 571-8686, Japan.

In the present study, approximately 300 *PVTx* properties including those at the bubble points of the three binary systems propane (1) + *n*-butane (2), propane (1) + isobutane (3), and *n*-butane (2) + isobutane (3) were measured by using a vibrating-tube densimeter apparatus. Nearly the same number of data were also obtained for the ternary system propane (1) + *n*-butane (2) + isobutane (3). The measurement system has been reported by the present authors[7] and has been used for pure refrigerant measurements, including those for hydrofluoroethers[8] and hydrocarbons.[9] The *PVTx* data were compared with the available mixture models. The representation of the saturated-liquid densities is also discussed in this paper.

On the basis of the present measurements, we have proposed a new mixing rule for a liquid-phase thermodynamic model that was originally developed by us.[9] In addition to the comparison with the available *PVTx* data, the thermodynamic consistency of the model is also disucussed by presenting some derived properties including the compressibility, specific heat capacity, and speed of sound.

Setup. A *PVT* property measurement system with a vibrating-tube densimeter was used in the present study. The apparatus is described in the literature[7,10] in detail.

The system configuration of the present apparatus is illustrated in Figure 1. The system has a pressure−density measurement unit shown in Figure 2 as a main part. A commercially available densimeter (DMA512, Anton Paar, K. G.) was attached to a stainless steel block being applied as a balance weight (5.5 kg). It was suspended from the mounting frame of the apparatus. There were also a digital pressure gauge (PT) and a variable-volume vessel (VB) installed between some of the valves.

The sample pressure and density can be controlled through the metallic bellows of the variable-volume vessel by injecting or releasing nitrogen gas into and from the outer space of the bellows.

A standard platinum resistance thermometer (PRT) was installed very close to the densimeter. The temperature was regarded as being uniform by circulating the bath fluid (silicone oil), and it was feedback controlled by tempera-

10.1021/je049671t CCC: $30.25
Published on Web 01/14/2005

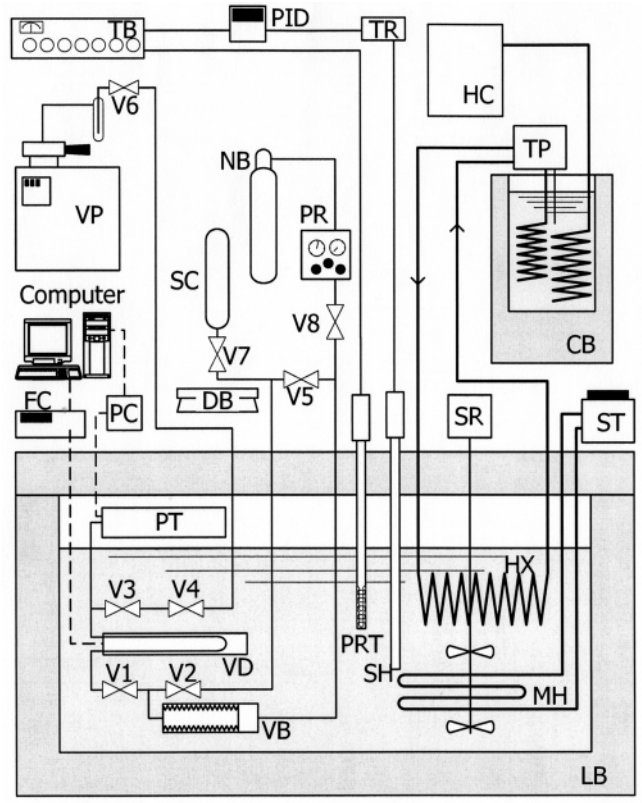

Figure 1. Schematic diagram of the experimental apparatus: VD, vibrating-tube densimeter cell; FC, frequency counter; PT, digital pressure gauge; PC, pressure computer; VB, variable-volume vessel with metallic bellows; PR, pressure regulator; NB, nitrogen gas bomb; SC, sample-supplying cylinder; DB, digital balance; VP, vacuum pump; PRT, standard platinum resistance thermometer; TB, thermometer bridge; LB, liquid bath; PID, PID controller; TR, thyristor regulator; SH, subheater; MH, main heater; ST, slide transformer; SR, stirrer; HX, heat exchanger; TP, temperature regulator pump; CB, cooling bath; HC, handy cooler; V1−7, valves.

ture-controlling devices such as a PID controller (PID), a thermometer bridge (TB), and a subheater (SH).

Materials and Mixture Sample Charging. In the present study, the mixture sample was prepared from each pure component sample as follows. Research-grade-purity samples of propane, *n*-butane, and isobutane were supplied by Nippon Sanso Co., who had reported their purity to be 99.99 mol % or higher from their gas-chromatograph analysis.

Each pure sample of previously planned mass (3 to 15 g) was prepared in a sample-supplying cylinder. The evacuated cylinder was charged with each pure sample, and then the mass of the cylinder was measured and regulated with an electronic balance with 1 mg resolution. Then, two or three sample cylinders prepared as described above were connected to the density measurement system as shown in Figure 3. For mixture sample charging, it is essential to let all of the prepared sample transfer into the measurement system in order to conduct density measurements with the same composition sample as prepared. Because a flushing procedure was not available, it was necessary to evacuate the system and sample feeding line under extreme vacuum for several hours. It was possible to conduct a flushing procedure with a sample of one of the mixture components and it was separately prepared from those used for the measurement.

After a considerable period of evacuation, valve V3 was closed, and then the sample-supplying cylinder valves were

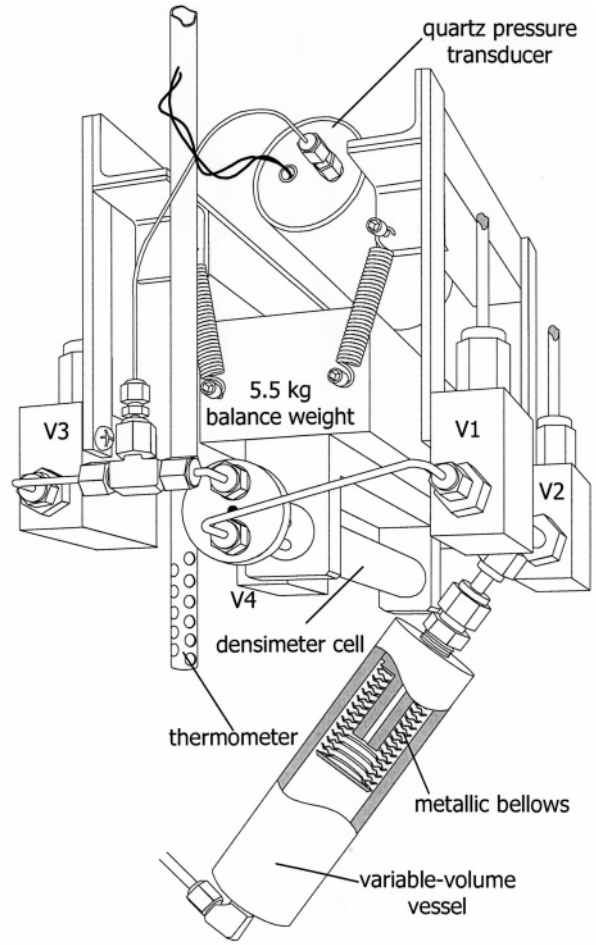

Figure 2. Drawing of the pressure−density measurement unit.

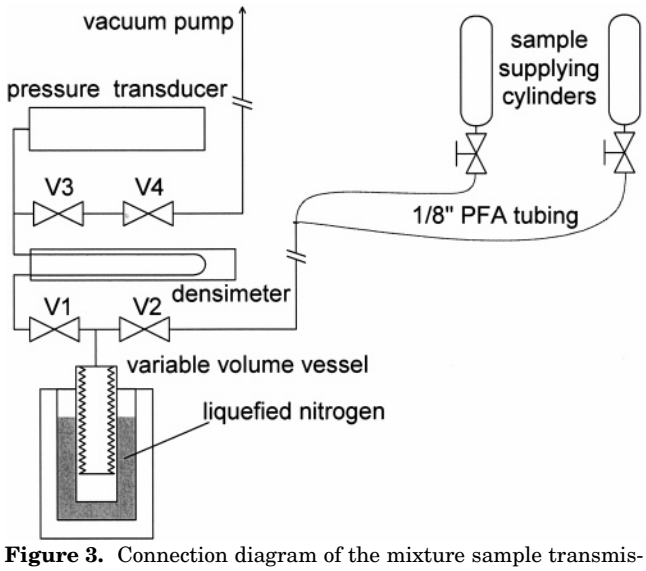

Figure 3. Connection diagram of the mixture sample transmission procedure.

opened to let the sample transfer into the system. To charge the measurement system with the entire sample, the variable-volume vessel was cooled by immersing it into liquefied nitrogen while the liquid bath was lowered. In this manner, the whole sample was condensed or solidified inside the bellows. In addition, to make the remaining sample evaporate and be extracted from the sample-supplying cylinder, it was heated with a heating bulb.

Bubble-Point Measurement. By employing the new procedure proposed, we determined the bubble point as

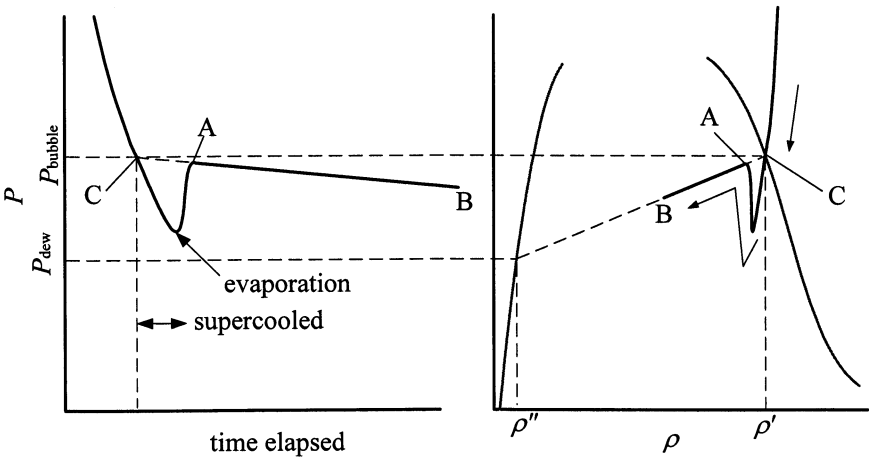

Figure 4. Pressure behavior in the vicinity of the bubble point during gradual expansion.

follows. Namely, in the liquid phase in the vicinity of the bubble point, the sample pressure was slowly lowered by slightly opening valve V8 in Figure 1 and extracting the nitrogen gas. A suitable pressure-dropping rate is about -1 to -10 kPa·min^{-1}. When the pressure went down below the bubble-point pressure, the mixture sample became supercooled until sudden evaporation occurs by a certain reason. Once the evaporation happened, it continued until the pressure recovered to a normal level, and then it gradually descended along the isotherm under the two-phase condition.

This behavior is illustrated in Figure 4. Ideally, the isothermal pressure line kinks at bubble point C in Figure 4 and then goes straight along the two-phase isothermal pressure line C−A−B to point B. In reality, however, bubble point C is located at the intersection point with the extension of straight line A−B. However, the sample temperature is lower because the pressure is decreasing. Therefore, in the present study, two or three apparent intersection points were observed with a different pressure-dropping rate, and thus the bubble point was determined precisely by extrapolating to the state point where $dP/dt = 0$ (t: time elapsed).

Calibration and Uncertainty. The temperature measurement uncertainty was 3 mK, with a coverage factor of $k = 2$. The value is a sum of the measurement uncertainty of the thermometer (PRT), the thermometer bridge (TB) and of the temperature fluctuation of the PID control (±1 mK). At 360 K or higher, it became 7 mK because of an increase in temperature fluctuations.

We have estimated the pressure measurement uncertainty to be $U = 0.26$ kPa + $0.00022P$. Because the digital pressure gauge is placed inside the liquid bath, it was calibrated over the full range of temperature (240 to 380) K. The nonlinearity of the pressure gauge was also calibrated.

When calibrating a vibrating-tube densimeter, one must be careful because the density measurement uncertainty may increase at a certain difference in density from the calibration point because the relation between the vibration period and the density is not perfectly linear. This is particularly a problem when measuring the density of hydrocarbons whose density is about (400 to 600) kg·m^{-3} in the liquid phase. In the present study, we have corrected the nonlinearlity of the densimeter by employing the following calibration function (eq 1).

This function was determined by measuring the vibration period of water. The nonlinearity of the relation between τ^2 and ρ is corrected by introducing a device-dependent constant, μ,

$$\rho = A\frac{(1+\mu)x}{1-\mu x} \tag{1}$$

$$\mathrm{A} = (a_1 + a_2 T^{*0.75} + a_3 T^{*3})(1 - a_4 P^{*}) \tag{2}$$

$$P^{*} = \frac{P/\mathrm{kPa}}{7000} \tag{3}$$

$$T^{*} = \frac{T/\mathrm{K}}{400} \tag{4}$$

where x is a periodical parameter defined by $x = (\tau^2/\tau_0^2) - 1$, τ denotes a vibration period, and τ_0 is that under vacuum. The parameter τ_0 was measured under vacuum condition between each isothermal experiment for the sample. A proportional parameter, A, was determined by calibration with water, where μ was determined to be $\mu = 0.0030 \pm 0.0005$ by comparing the density of water and isooctane, whose density is precisely calibrated to 40 ppm on the same (P, T) grid. The density measurement uncertainty was evaluated to be 0.1 kg·m^{-3} + 0.00024ρ, where the coverage factor is $k = 2$.

The uncertainty in mole fraction was estimated from the mass measurement uncertainty (1 mg) in the mixture sample preparation procedure to be less than 0.1 mol %.

Results and Discussion

Introductory Remarks. A total of 288, 271, and 313 liquid-phase *PVTx* properties for binary systems propane (1) + *n*-butane (2), propane (1) + isobutane (3), and *n*-butane (2) + isobutane (3) were obtained for mole fractions of 0.25, 0.50, and 0.75. We have also measured 295 *PVTx* values of the ternary system propane (1) + *n*-butane (2) + isobutane (3) in the liquid phase at mole fractions (x_1, x_2) = (0.2, 0.6), (0.33, 0.34), and (0.6, 0.2). These data are tabulated in Tables 1 through 4. Bubble-point pressures and saturated-liquid densities were also obtained, and these data are summarized in Table 5. The composition distribution of the measured data are illustrated in a trilinear diagram (Figure 5) together with other reported *PVTx* data. It should be noted that a couple of data points reported by Luo and Miller[11] are gas-phase *PVTx* data. It is emphasized, therefore, that the present data contain the first set of liquid-phase *PVTx* data for the ternary mixture of present interest.

Table 1. Experimental Liquid Phase *PVTx* Data for the Binary System Propane (1) + *n*-Butane

T	*P*	ρ	*T*	*P*	ρ	*T*	*P*	ρ	*T*	*P*	ρ	*T*	*P*	ρ	*T*	*P*	ρ
K	kPa	kg·m^{-3}	K	kPa	kg·m^{-3}	K	kPa	kg·m^{-3}	K	kPa	kg·m^{-3}	K	kPa	kg·m^{-3}	K	kPa	kg·m^{-3}
				$x_1 = 0.250$									$x_1 = 0.500$				
239.039	6930.6	629.26	239.039	6518.0	628.86	239.039	6029.4	628.39	300.000	5508.8	545.86	300.000	4953.2	544.76	300.000	4514.7	543.88
239.039	5524.3	627.90	239.039	4950.0	627.33	239.039	4514.6	626.90	300.000	4015.9	542.85	300.000	3505.6	541.79	300.000	2946.2	540.60
239.039	3994.0	626.39	239.039	3473.7	625.88	239.039	3058.3	625.46	300.000	2461.4	539.56	300.000	1950.9	538.44	300.000	1541.4	537.52
239.039	2486.4	624.89	239.039	1962.4	624.35	239.039	1507.7	623.90	300.000	990.0	536.26	320.000	7116.4	524.52	320.000	6479.5	522.98
239.039	943.7	623.31	239.039	463.7	622.82	260.000	7011.2	608.56	320.000	5989.8	521.77	320.000	5490.6	520.51	320.000	4988.6	519.21
260.000	6503.8	607.98	260.000	6034.1	607.43	260.000	5512.4	606.82	320.000	4497.4	517.90	320.000	4017.1	516.60	320.000	3509.2	515.19
260.000	5017.7	606.24	260.000	4511.7	605.63	260.000	4007.0	605.01	320.000	2999.8	513.74	320.000	2516.5	512.32	320.000	2010.3	510.79
260.000	3449.6	604.34	260.000	3004.0	603.79	260.000	2521.3	603.20	320.000	1496.3	509.20	340.000	7014.4	497.66	340.000	6534.4	496.09
260.000	1989.9	602.54	260.000	1482.5	601.91	260.000	1004.9	601.30	340.000	6031.2	494.40	340.000	5511.6	492.60	340.000	5012.2	490.80
260.000	524.1	600.69	280.000	7009.3	587.89	280.000	6517.1	587.21	340.000	4496.8	488.89	340.000	4016.2	487.04	340.000	3515.5	485.04
280.000	6005.9	586.49	280.000	5502.7	585.78	280.000	5019.7	585.09	340.000	3013.6	482.96	340.000	2508.8	480.75	340.000	2013.6	478.50
280.000	4505.3	584.35	280.000	4015.0	583.63	280.000	3502.3	582.88	360.000	6972.7	468.36	360.000	6530.6	466.12	360.000	6017.8	463.52
280.000	3000.3	582.13	280.000	2503.9	581.38	280.000	2015.5	580.63	360.000	5525.0	460.95	360.000	5025.4	458.22	360.000	4529.2	455.37
280.000	1496.7	579.83	280.000	994.1	579.05	280.000	524.1	578.30	360.000	4023.8	452.26	360.000	3530.7	449.00	360.000	3014.4	445.35
300.000	7074.7	566.49	300.000	6488.8	565.48	300.000	5929.8	564.50	360.000	2528.0	441.58	380.000	6908.8	431.30	380.000	6480.6	428.09
300.000	5451.1	563.65	300.000	5031.0	562.90	300.000	4511.3	561.97	380.000	5962.5	423.89	380.000	5494.5	419.73	380.000	5019.0	415.08
300.000	3998.7	561.02	300.000	3507.9	560.13	300.000	3012.5	559.20	380.000	4476.5	409.03	380.000	4001.1	402.87	380.000	3523.1	395.46
300.000	2497.9	558.21	300.000	2002.5	557.25	300.000	1504.4	556.28					$x_1 = 0.750$				
300.000	1005.5	555.26	320.000	7003.8	543.49	320.000	6524.6	542.42	240.000	7045.6	597.30	240.000	6539.6	596.77	240.000	6044.8	596.20
320.000	6013.9	541.36	320.000	5501.0	540.19	320.000	4989.7	539.00	240.000	5521.6	595.64	240.000	4946.9	594.99	240.000	4526.8	594.51
320.000	4472.0	537.80	320.000	4012.1	536.73	320.000	3516.7	535.58	240.000	4031.2	593.97	240.000	3519.4	593.39	240.000	3022.7	592.80
320.000	3012.6	534.34	320.000	2502.8	533.06	320.000	1996.7	531.76	240.000	2519.5	592.21	240.000	2024.2	591.63	240.000	1505.4	591.03
320.000	1482.2	530.41	320.000	997.4	529.12	340.000	6991.8	518.67	240.000	1006.3	590.44	240.000	514.9	589.83	260.000	6943.0	575.60
340.000	6477.8	517.22	340.000	5958.5	515.74	340.000	5479.2	514.33	260.000	6498.8	575.04	260.000	6049.2	574.41	260.000	5508.1	573.69
340.000	4981.8	512.84	340.000	4514.8	511.39	340.000	3984.5	509.71	260.000	5022.8	573.01	260.000	4494.5	572.27	260.000	4006.2	571.62
340.000	3488.0	508.09	340.000	2997.6	506.44	340.000	2454.3	504.54	260.000	3495.5	570.88	260.000	3015.6	570.19	260.000	2508.4	569.45
340.000	1990.9	502.87	340.000	1485.3	500.98	360.000	6966.9	491.30	260.000	2003.6	568.71	260.000	1504.2	567.97	260.000	996.9	567.21
360.000	6472.2	489.44	360.000	5999.9	487.58	360.000	5492.3	485.53	260.000	489.6	566.44	280.000	7012.2	553.04	280.000	6530.4	552.22
360.000	5018.1	483.52	360.000	4494.7	481.23	360.000	4004.6	478.98	280.000	6043.7	551.39	280.000	5508.8	550.50	280.000	4984.9	549.59
360.000	3479.5	476.45	360.000	3030.5	474.17	360.000	2483.2	471.24	280.000	4508.2	548.75	280.000	4015.0	547.86	280.000	3513.7	546.96
360.000	1968.3	468.30	380.000	6952.8	459.99	380.000	6502.4	457.46	280.000	3018.4	546.06	280.000	2509.6	545.11	280.000	2012.9	544.18
380.000	5995.5	454.49	380.000	5497.5	451.38	380.000	4998.7	448.08	280.000	1506.3	543.19	300.000	7015.2	529.08	300.000	6473.6	527.92
380.000	4501.1	444.52	380.000	3998.7	440.67	380.000	3508.7	436.48	300.000	5950.0	526.78	300.000	5474.7	525.74	300.000	5016.7	524.69
380.000	3006.4	431.76	380.000	2507.8	426.44				300.000	4513.8	523.55	300.000	4017.5	522.39	300.000	3511.5	521.18
				$x_1 = 0.500$					300.000	3009.2	519.95	300.000	2507.7	518.69	300.000	1972.1	517.33
240.000	6973.1	613.74	240.000	6502.7	613.25	240.000	6000.1	612.74	300.000	1504.7	516.09	300.000	1002.3	514.75	320.000	7020.7	502.78
240.000	5472.1	612.19	240.000	4972.1	611.66	240.000	4493.1	611.14	320.000	6522.9	501.37	320.000	6001.7	499.85	320.000	5520.4	498.43
240.000	3952.5	610.58	240.000	3501.4	610.09	240.000	2956.0	609.51	320.000	5019.1	496.89	320.000	4512.7	495.29	320.000	4013.7	493.68
240.000	2491.6	609.00	240.000	1962.4	608.42	240.000	1479.0	607.88	320.000	3459.5	491.82	320.000	3011.6	490.26	320.000	2497.1	488.41
240.000	996.7	607.38	240.000	478.5	606.78	260.000	6986.6	593.49	320.000	2020.7	486.64	320.000	1509.8	484.66	340.000	6953.2	472.85
260.000	6512.1	592.90	260.000	6015.4	592.29	260.000	5513.7	591.66	340.000	6495.0	471.01	340.000	5990.2	468.91	340.000	5517.0	466.87
260.000	5017.4	591.03	260.000	4525.9	590.39	260.000	4004.5	589.73	340.000	4991.2	464.48	340.000	4469.1	462.01	340.000	4021.6	459.81
260.000	3506.0	589.10	260.000	3014.9	588.45	260.000	2517.2	587.78	340.000	3542.6	457.27	340.000	3018.0	454.37	340.000	2527.2	451.44
260.000	2004.6	587.10	260.000	1506.4	586.42	260.000	1001.1	585.74	340.000	1994.9	448.06	360.000	6960.2	436.27	360.000	6494.0	433.30
260.000	495.8	585.02	280.000	6972.3	571.72	280.000	6507.4	571.01	360.000	5965.8	429.75	360.000	5477.4	426.13	360.000	4959.4	422.10
280.000	6009.4	570.25	280.000	5506.3	569.47	280.000	4998.7	568.69	360.000	4499.5	418.08	360.000	4034.2	413.59	360.000	3504.1	407.74
280.000	4524.6	567.93	280.000	4016.7	567.11	280.000	3504.2	566.28	360.000	2981.1	400.91	380.000	6897.6	390.75	380.000	6503.9	386.32
280.000	3006.4	565.46	280.000	2501.9	564.62	280.000	2004.1	563.79	380.000	5986.2	379.48	380.000	5491.2	371.58	380.000	5025.3	362.30
280.000	1503.2	562.93	280.000	996.1	562.05	280.000	533.2	561.24	380.000	4538.7	349.07						
300.000	6959.9	548.68	300.000	6466.1	547.72	300.000	5953.0	546.73									

Binary System Propane (1) + n-Butane (2). The measured data for the binary system propane (1) + *n*-butane (2) are illustrated on a *P*−*T* diagram (Figure 6) together with other literature data. There are two major data sets by Holcomb et al.[12] and Parrish.[13] A few points were reported by Kahre[14] and Thompson and Miller.[15] Luo and Miller[11] reported a single datum point at 15 °C.

Data by Holcomb et al.[12] are limited to a single mole fraction, and the temperature range of those by Parrish[13] are (10 to 60) °C; therefore, the present measurements contain the first set of data at extended temperatures for several mole fractions.

The available density data were compared with the mixture models of Lemmon and Jacobsen[5] (LJ) and Miyamoto and Watanabe[6] (MW).

Figure 7 shows the relative deviations in the density data for the binary system propane (1) + *n*-butane (2) from the LJ model (top side) and from the MW model (bottom). It is seen from these deviation plots that both mixture models show nearly the same representation for liquid densities. Most of the data below 360 K are well represented within ±0.3%, but the deviation increases to ±0.8% at higher temperatures. Because the data of both Holcomb et al.[12] and this work ($x_1 = 0.250$) show the same positive deviation at temperatures from (360 to 380) K, it is considered that the large scatter in the higher-temperature region is a characteristic of the thermodynamic models.

The saturated-liquid density data for the binary system propane (1) + *n*-butane (2) are also compared with the two models in Figure 8. There are several series of saturated-liquid density measurements only for the present binary system, among all possible combinations of binary and ternary mixtures of propane, *n*-butane, and isobutane. In this comparison of the data with the models, there is a large spread in the density deviations of more than ±5% around 400 K that are close to the critical-point temperature, but the vertical maximum scale is limited to ±1% in order to discuss the detailed comparison. As seen in Figure 8, the present data agree well with the LJ model within ±0.14% and ±0.10% from the MW model except for two points. The maximum deviation of the present data are found for the measurement at 360 K, $x_1 = 0.750$, being −0.72% from the LJ model and −0.60% from the MW model, and it is not larger than the deviation of other literature data.

Binary System Propane (1) + Isobutane (3). Figure 9 illustrates the *PVTx* data distribution for the binary

Table 2. Experimental Liquid Phase *PVTx* Data for the Binary System Propane (1) + Isobutane (3)

T	P	ρ	T	P	ρ	T	P	ρ	T	P	ρ	T	P	ρ	T	P	ρ
K	kPa	kg·m^{-3}	K	kPa	kg·m^{-3}	K	kPa	kg·m^{-3}	K	kPa	kg·m^{-3}	K	kPa	kg·m^{-3}	K	kPa	kg·m^{-3}
$x_1 = 0.250$												$x_1 = 0.499$					
240.000	6987.7	615.48	240.000	6541.5	615.00	240.000	6033.0	614.45	300.000	3043.4	528.93	300.000	2530.4	527.70	300.000	2026.1	526.45
240.000	5533.4	613.91	240.000	5030.4	613.37	240.000	4519.1	612.81	300.000	1519.6	525.17	300.000	996.8	523.82	320.000	6930.3	511.85
240.000	4027.7	612.28	240.000	3537.9	611.73	240.000	3028.4	611.15	320.000	6524.9	510.74	320.000	5997.3	509.24	320.000	5545.8	507.90
240.000	2533.0	610.61	240.000	2004.5	610.02	240.000	1505.9	609.45	320.000	4954.2	506.17	320.000	4530.4	504.90	320.000	4037.4	503.38
240.000	1000.1	608.87	240.000	475.1	608.27	240.000	398.2	608.19	320.000	3550.0	501.84	320.000	3023.9	500.12	320.000	2488.7	498.31
260.000	7006.2	595.15	260.000	6474.3	594.47	260.000	6051.9	593.96	320.000	2041.5	496.75	320.000	1461.2	494.61	340.000	7045.5	482.76
260.000	5550.8	593.30	260.000	4976.3	592.53	260.000	4476.3	591.87	340.000	6513.0	480.75	340.000	5982.0	478.68	340.000	5450.5	476.50
260.000	3986.7	591.20	260.000	3517.2	590.65	260.000	2995.0	589.98	340.000	4990.6	474.50	340.000	4508.4	472.34	340.000	4012.5	470.04
260.000	2504.8	589.32	260.000	2004.4	588.63	260.000	1481.6	587.88	340.000	3485.7	467.47	340.000	2981.6	464.85	340.000	2456.0	461.99
260.000	990.2	587.20	260.000	521.1	586.55	280.000	6965.6	573.82	340.000	2002.6	459.37	360.000	6977.0	452.14	360.000	6487.4	449.41
280.000	6968.2	573.78	280.000	6532.5	573.13	280.000	5989.4	572.28	360.000	5992.3	446.54	360.000	5436.6	443.06	360.000	5000.3	440.17
280.000	5485.0	571.47	280.000	4979.1	570.66	280.000	4516.8	569.91	360.000	4488.6	436.48	360.000	3988.8	432.58	360.000	3496.3	428.34
280.000	3992.4	569.03	280.000	3488.8	568.19	280.000	2999.1	567.36	360.000	2996.3	423.54	360.000	2495.4	418.03	380.000	6885.8	412.58
280.000	2513.6	566.51	280.000	2007.8	565.62	280.000	1462.8	564.67	380.000	6422.5	408.17	380.000	5943.1	403.16	380.000	5506.7	398.06
280.000	1004.7	563.86	280.000	500.3	562.94	300.000	6957.0	551.23	380.000	5016.0	391.43	380.000	4501.9	383.09	380.000	4047.9	373.76
300.000	6516.0	550.41	300.000	6025.1	549.47	300.000	5511.8	548.38	380.000	3540.7	358.66						
300.000	5016.4	547.38	300.000	4483.4	546.25	300.000	4012.0	545.28				$x_1 = 0.750$					
300.000	3488.8	544.16	300.000	3014.6	543.13	300.000	2510.6	542.01	240.000	6969.5	592.10	240.000	6541.0	591.59	240.000	6009.0	590.98
300.000	2006.6	540.87	300.000	1503.7	539.71	300.000	1001.6	538.53	240.000	5496.4	590.37	240.000	4996.8	589.79	240.000	4515.3	589.21
320.000	6964.1	526.60	320.000	6479.8	525.39	320.000	6001.8	524.19	240.000	4012.9	588.63	240.000	3545.4	588.06	240.000	3006.4	587.40
320.000	5517.3	522.93	320.000	4990.1	521.53	320.000	4522.1	520.26	240.000	2531.8	586.84	240.000	2000.7	586.19	240.000	1473.4	585.53
320.000	4022.9	518.87	320.000	3508.1	517.40	320.000	3007.6	515.95	240.000	1024.1	584.98	240.000	529.1	584.35	260.000	251.9	560.57
320.000	2522.2	514.49	320.000	2023.3	512.94	320.000	1500.0	511.28	260.000	6922.9	570.57	260.000	6513.6	570.10	260.000	5537.1	568.72
320.000	1020.5	509.69	340.000	6963.0	500.75	340.000	6527.5	499.31	260.000	4968.6	568.07	260.000	4527.2	567.50	260.000	4039.9	566.81
340.000	6022.3	497.59	340.000	5522.3	495.84	340.000	4964.9	493.81	260.000	3494.1	566.00	260.000	3035.5	565.31	260.000	2508.8	564.52
340.000	4503.0	492.08	340.000	4015.7	490.21	340.000	3532.9	488.26	260.000	2030.6	563.80	260.000	1524.1	563.04	260.000	1026.1	562.22
340.000	3027.2	486.13	340.000	2523.8	483.92	340.000	2028.0	481.60	260.000	527.0	561.44	280.000	478.7	535.35	280.000	6931.1	547.66
340.000	1514.2	479.11	360.000	6956.4	471.48	360.000	6444.6	469.09	280.000	6488.2	546.89	280.000	6012.9	546.05	280.000	5530.9	545.19
360.000	5982.9	466.86	360.000	5515.2	464.45	360.000	4983.9	461.58	280.000	4965.2	544.17	280.000	4544.4	543.38	280.000	4026.3	542.43
360.000	4520.2	458.95	360.000	4022.3	455.95	360.000	3519.8	452.71	280.000	3522.3	541.47	280.000	3019.4	540.50	280.000	2510.3	539.50
360.000	3022.3	449.26	360.000	2532.9	445.56	360.000	2023.3	441.34	280.000	2029.6	538.54	280.000	1517.2	537.51	280.000	990.6	536.42
380.000	7060.8	437.93	380.000	6471.8	433.74	380.000	5972.1	429.89	300.000	824.3	507.35	300.000	6954.6	522.99	300.000	6473.0	521.92
380.000	5488.5	425.84	380.000	5019.6	421.52	380.000	4453.9	415.70	300.000	5960.9	520.74	300.000	5458.9	519.57	300.000	4994.5	518.46
380.000	3969.5	409.99	380.000	3495.5	403.43	380.000	2977.2	394.60	300.000	4467.1	517.17	300.000	3996.7	515.97	300.000	3519.2	514.75
$x_1 = 0.499$									300.000	3028.7	513.47	300.000	2493.2	512.04	300.000	2028.3	510.77
250.000	6818.8	592.84	250.000	6509.5	592.48	250.000	5996.5	591.90	300.000	1534.0	509.38	320.000	1325.3	475.52	320.000	7044.7	496.03
250.000	5484.6	591.29	250.000	5042.2	590.74	250.000	4532.5	590.12	320.000	6495.0	494.38	320.000	6003.6	492.85	320.000	5527.2	491.33
250.000	3995.9	589.47	250.000	3492.5	588.84	250.000	3012.9	588.23	320.000	4968.0	489.50	320.000	4507.7	487.92	320.000	3994.2	486.12
250.000	2489.8	587.55	250.000	2027.5	586.95	250.000	1511.1	586.26	320.000	3506.4	484.35	320.000	3025.6	482.53	320.000	2517.7	480.54
250.000	1014.4	585.61	250.000	515.5	584.94	280.000	6938.9	560.98	320.000	2021.1	478.51	320.000	1505.3	476.31	340.000	7081.1	466.25
280.000	6525.9	560.31	280.000	6027.0	559.46	280.000	5482.8	558.54	340.000	6506.1	463.79	340.000	5960.4	461.33	340.000	5511.1	459.22
280.000	5014.0	557.72	280.000	4518.6	556.87	280.000	3992.0	555.95	340.000	4963.1	456.51	340.000	4498.6	454.09	340.000	3969.0	451.17
280.000	3519.6	555.10	280.000	3022.9	554.21	280.000	2489.1	553.22	340.000	3510.1	448.46	340.000	3027.4	445.39	340.000	2489.8	441.74
280.000	2007.8	552.34	280.000	1514.0	551.39	280.000	952.8	550.30	360.000	6932.1	431.05	360.000	6509.8	428.41	360.000	5932.0	424.33
280.000	467.2	549.36	300.000	6984.7	537.69	300.000	6517.3	536.72	360.000	5456.3	420.47	360.000	4923.7	415.42	360.000	4484.8	411.08
300.000	5975.7	535.56	300.000	5458.6	534.46	300.000	4958.9	533.34	360.000	3971.4	405.35	360.000	3960.0	405.21	360.000	3518.2	399.53
300.000	4503.6	532.34	300.000	3995.5	531.16	300.000	3486.8	529.95									

system propane (1) + isobutane (3). Most of the data are reported by Duarte-Garza and Magee,[16] except for 4 points by Thompson et al.[15] and 19 points by Kahre.[14]

Density deviations of these available data from those calculated by the LJ model and the MW model are shown in Figure 10. The deviation plots show that both mixture models have nearly the same reproducibility for the present measured data, within about ±0.7%. The data and the models agree well within ±0.3%, but the deviations increase at higher temperatures. The present data have larger scatter than those by Duarte-Garza and Magee,[16] probably because of the closer adherence of the present data to the saturation boundary. As for the data by Duarte-Garza and Magee,[16] the LJ model reproduces the data within ±0.2%. The maximum deviation of their data from the MW model is about 0.04%, which is smaller than the experimental uncertainty of the data.

Saturated liquid densities were also compared with the mixture models as illustrated in Figure 11. The present measured data have deviations within ±0.5% except for a single datum. It is considered to be satisfactory because the density expectation uncertainty should be larger than that of the models for pure fluids.

Binary System n-Butane (2) + Isobutane (3). Figure 12 illustrates the *PVTx* data distribution for the binary system *n*-butane (2) + isobutane (3). In contrast to the other two binary systems, there are not enough experimental data for this system, probably because the system draws less interest becaus of the ideality of the binary system of these similar molecules. Only Kahre[14] has reported 16 data points at relatively low pressures (from 0.2 to 0.7) MPa. To develop a precise thermodynamic model for mixture systems including *n*-butane and isobutane, however, experimental data for this binary system are still important. The present data are the first report of a wide range set of *PVTx* data, which can offer valuable information.

The experimental *PVTx* data for *n*-butane (2) + isobutane (3) are compared with the LJ and the MW models in Figure 13. The data of this work deviate by (−0.1 to 0.25)% from the LJ model and by (−0.56 to 0.20)% from the MW model. One reason that the agreement between the data and the models is better than that of the other two binary systems may be the ideality of this binary system as described above. Another is that the experimental range (up to 380 K) is considerably lower than the critical temperatures of *n*-butane (2) (425.125 K[17]) and isobutane (3) (407.761 K[18]).

The saturated liquid densities for this binary system are also compared with those for the LJ and the MW models,

Table 3. Experimental Liquid Phase *PVTx* Data for the Binary System *n*-Butane (2) + Isobutane (3)

T/K	P/kPa	ρ/kg·m^{-3}	T/K	P/kPa	ρ/kg·m^{-3}	T/K	P/kPa	ρ/kg·m^{-3}	T/K	P/kPa	ρ/kg·m^{-3}	T/K	P/kPa	ρ/kg·m^{-3}	T/K	P/kPa	ρ/kg·m^{-3}
$x_2 = 0.250$									$x_2 = 0.500$								
240.000	6977.0	628.56	240.000	6517.4	628.10	240.000	6067.5	627.64	300.000	983.9	560.78	300.000	510.2	559.82	300.000	312.0	559.40
240.000	5519.2	627.11	240.000	5024.9	626.58	240.000	4485.6	626.03	320.000	7093.8	549.62	320.000	6462.7	548.28	320.000	5971.8	547.22
240.000	3970.1	625.50	240.000	3481.8	624.99	240.000	2987.3	624.47	320.000	5465.3	546.12	320.000	4992.4	545.07	320.000	4492.1	543.94
240.000	2493.8	623.95	240.000	2001.8	623.43	240.000	1503.1	622.90	320.000	3972.8	542.72	320.000	3465.4	541.53	320.000	3020.8	540.47
240.000	999.5	622.36	240.000	481.6	621.79	260.000	7000.3	608.81	320.000	2513.8	539.22	320.000	2007.9	537.95	320.000	1594.1	536.89
260.000	6519.2	608.25	260.000	6028.5	607.65	260.000	5506.4	607.02	320.000	978.9	535.28	340.000	7084.7	525.72	340.000	6476.8	524.07
260.000	5023.4	606.44	260.000	4521.0	605.82	260.000	4014.1	605.19	340.000	6016.6	522.80	340.000	5502.0	521.34	340.000	4988.5	519.84
260.000	3505.2	604.56	260.000	2999.7	603.92	260.000	2511.6	603.29	340.000	4526.2	518.46	340.000	4042.3	516.97	340.000	3521.9	515.35
260.000	2003.1	602.64	260.000	1490.8	601.97	260.000	979.3	601.29	340.000	3001.4	513.65	340.000	2527.9	512.06	340.000	2008.5	510.27
260.000	503.7	600.66	280.000	6984.1	588.18	280.000	6510.8	587.50	340.000	1561.3	508.67	340.000	998.6	506.59	360.000	7022.1	499.47
280.000	6024.7	586.78	280.000	5523.8	586.04	280.000	5006.3	585.27	360.000	6511.4	497.56	360.000	6019.4	495.75	360.000	5508.6	493.77
280.000	4504.4	584.53	280.000	4008.0	583.74	280.000	3506.9	582.98	360.000	5018.9	491.80	360.000	4510.2	489.71	360.000	4019.1	487.57
280.000	3023.0	582.23	280.000	2512.7	581.42	280.000	2009.2	580.63	360.000	3511.2	485.28	360.000	3005.9	482.91	360.000	2525.0	480.50
280.000	1496.0	579.79	280.000	997.5	578.99	280.000	491.4	578.14	360.000	2018.5	477.84	360.000	1517.3	475.07	380.000	6981.4	469.94
300.000	7001.6	566.76	300.000	6498.0	565.90	300.000	6036.6	565.05	380.000	6505.2	467.52	380.000	6010.6	464.88	380.000	5511.6	462.08
300.000	5514.6	564.10	300.000	5016.3	563.17	300.000	4513.9	562.25	380.000	5001.3	459.04	380.000	4521.7	456.00	380.000	4015.3	452.56
300.000	4007.7	561.28	300.000	3510.6	560.33	300.000	3014.0	559.36	380.000	3519.0	448.92	380.000	3005.0	444.82	380.000	2506.6	440.41
300.000	2498.6	558.33	300.000	1997.4	557.29	300.000	1497.1	556.26	$x_2 = 0.750$								
300.000	999.4	555.23	300.000	502.9	554.17	320.000	7034.9	544.07	240.000	6991.5	637.75	240.000	6492.4	637.29	240.000	6023.5	636.82
320.000	6514.9	542.91	320.000	5970.9	541.67	320.000	5506.3	540.60	240.000	5515.8	636.31	240.000	5011.3	635.85	240.000	4509.6	635.35
320.000	4998.1	539.39	320.000	4485.3	538.17	320.000	4006.4	537.00	240.000	4015.3	634.92	240.000	3507.2	634.38	240.000	3003.9	633.91
320.000	3504.2	535.74	320.000	2989.3	534.40	320.000	2511.0	533.15	240.000	2505.1	633.43	240.000	2011.4	632.88	240.000	1500.2	632.38
320.000	2013.6	531.82	320.000	1496.2	530.40	320.000	1010.3	529.04	240.000	1001.0	631.85	240.000	499.0	631.33	260.000	7024.3	617.88
340.000	7019.9	519.55	340.000	6508.8	518.07	340.000	5999.1	516.58	240.000	6526.2	617.32	260.000	6004.4	616.79	260.000	5512.2	616.21
340.000	5500.3	515.08	340.000	4981.3	513.47	340.000	4508.6	511.95	240.000	5018.2	615.65	260.000	4519.2	615.15	260.000	4009.7	614.50
340.000	4004.8	510.31	340.000	3512.9	508.67	340.000	3009.8	506.91	260.000	3495.3	613.93	260.000	3016.5	613.40	260.000	2510.1	612.77
340.000	2495.8	505.08	340.000	2003.4	503.24	340.000	1510.0	501.39	260.000	2002.5	612.18	260.000	1489.5	611.52	260.000	993.2	610.92
360.000	7041.0	492.93	360.000	6497.2	490.83	360.000	6002.5	488.86	260.000	496.3	610.36	280.000	7039.4	597.80	280.000	6475.5	597.09
360.000	5503.6	486.78	360.000	5010.2	484.66	360.000	4493.0	482.35	260.000	5942.8	596.37	280.000	5525.5	595.77	280.000	4994.2	595.02
360.000	4007.3	480.03	360.000	3507.7	477.58	360.000	3010.1	474.99	260.000	4502.1	594.34	280.000	4010.5	593.64	280.000	3511.3	592.97
360.000	2482.6	472.10	360.000	1975.7	469.15	360.000	1523.6	466.34	280.000	3001.9	592.24	280.000	2501.0	591.51	280.000	1991.8	590.76
380.000	7003.2	462.28	380.000	6476.8	459.36	380.000	5986.7	456.50	280.000	1499.8	590.03	280.000	997.9	589.24	280.000	494.5	588.49
380.000	5481.2	453.35	380.000	5004.6	450.19	380.000	4463.2	446.33	280.000	7005.5	576.66	300.000	6473.1	575.78	300.000	5950.5	574.92
380.000	4000.0	442.76	380.000	3498.2	438.53	380.000	3007.8	433.95	280.000	5473.2	574.11	300.000	4997.8	573.31	300.000	4467.0	572.38
380.000	2496.5	428.54							300.000	4013.5	571.62	300.000	3483.6	570.68	300.000	2995.9	569.79
$x_2 = 0.500$									300.000	2510.2	568.90	300.000	2007.5	568.00	300.000	1493.0	567.04
240.000	6981.0	632.99	240.000	6486.1	632.50	240.000	5981.2	631.99	300.000	1002.4	566.11	300.000	505.7	565.16	320.000	7065.7	554.85
240.000	5486.4	631.50	240.000	4983.6	630.99	240.000	4467.2	630.47	300.000	6488.4	553.71	320.000	6015.9	552.74	320.000	5508.2	551.69
240.000	3982.7	629.98	240.000	3446.0	629.43	240.000	2976.4	628.95	300.000	4997.8	550.60	320.000	4515.1	549.56	320.000	3986.7	548.41
240.000	2468.8	628.43	240.000	1962.6	627.92	240.000	1472.5	627.41	320.000	3510.6	547.30	320.000	2990.8	546.14	320.000	2503.8	545.03
240.000	989.5	626.90	240.000	468.1	626.35	260.000	6987.3	613.20	320.000	2006.0	543.82	320.000	1506.1	542.64	320.000	1008.4	541.40
260.000	6531.1	612.67	260.000	6023.0	612.08	260.000	5517.9	611.47	340.000	7019.3	531.33	340.000	6496.3	529.99	340.000	5973.6	528.61
260.000	5026.4	610.89	260.000	4508.9	610.27	260.000	3991.1	609.66	340.000	5515.9	527.37	340.000	4990.6	525.87	340.000	4496.4	524.53
260.000	3514.0	609.08	260.000	2993.6	608.43	260.000	2507.6	607.84	340.000	4004.8	523.11	340.000	3499.6	521.61	340.000	3005.7	520.07
260.000	2010.9	607.22	260.000	1508.9	606.59	260.000	1011.2	605.96	340.000	2500.9	518.54	340.000	2020.5	516.97	340.000	1505.9	515.25
260.000	503.9	605.31	280.000	6953.9	592.89	280.000	6528.5	592.30	340.000	1008.5	513.55	360.000	7073.3	505.68	360.000	6484.4	503.73
280.000	5993.3	591.55	280.000	5479.3	590.82	280.000	5025.7	590.15	360.000	5964.2	501.91	360.000	5499.8	500.18	360.000	4948.8	498.12
280.000	4508.3	589.40	280.000	4012.8	588.67	280.000	3532.6	587.97	360.000	4443.6	496.16	360.000	3977.2	494.26	360.000	3489.3	492.24
280.000	3016.2	587.20	280.000	2510.6	586.43	280.000	1990.8	585.62	360.000	2961.3	489.97	360.000	2496.0	487.85	360.000	1976.3	485.36
280.000	1515.6	584.89	280.000	997.4	584.09	280.000	514.1	583.32	360.000	1517.1	483.05	380.000	6967.5	476.48	380.000	6475.4	474.16
300.000	7003.6	571.85	300.000	6511.5	571.01	300.000	5960.3	570.04	380.000	5998.4	471.80	380.000	5504.5	469.24	380.000	4994.0	466.44
300.000	5472.7	569.19	300.000	5026.1	568.40	300.000	4453.4	567.40	380.000	4476.8	463.44	380.000	4022.0	460.64	380.000	3482.8	457.09
300.000	3988.4	566.54	300.000	3476.1	565.59	300.000	3011.4	564.72	380.000	3014.5	453.77	380.000	2519.3	449.94	380.000	1992.3	445.43
300.000	2513.9	563.78	300.000	1992.8	562.77	300.000	1509.8	561.83									

as shown in deviation plots of Figure 14. The present experimental data show better agreement with the LJ model, within ±0.12%. Deviations from the MW model increase at higher temperatures by a maximum of −0.56% at 380 K.

Ternary System Propane (1) + n-Butane (2) + Isobutane (3). In Figure 15, the present measured *PVTx* data for the ternary system propane (1) + *n*-butane (2) + isobutane (3) are plotted. There are no *PVTx* data for the ternary system, other than two data points in the gas phase by Luo and Miller.[11]

The relative density deviations of the experimental data for the ternary system from the LJ and the MW models are illustrated in Figure 16. Although there are certain systematic deviation by up to −0.8% as the temperature rises to 380 K, it is recognized that most of the data are satisfactorily reproduced within ±0.3%. The agreement with the data and the MW model is considered to be good despite the fact that it was developed without any input data for the ternary system. The performance of the LJ and the MW models appears to be almost equivalent, but the internal dispersion of the data is smaller for the LJ model. Comparing the saturated liquid densities as shown in Figure 17, the experimental data are reproduced by the LJ and the MW model within ±0.3% below 340 K, but there are slightly larger systematic deviation by about ±0.4% found at higher temperatures.

Liquid-Density Equation

Functional Form and Mixing Rule. On the basis of the *PVTx* property data obtained in the present study, a mixture thermodynamic model for the liquid phase of the binary and ternary system composed of propane (1), *n*-butane (2), and isobutane (3) was develped. For the pure components, modified Tait equations of state (EoS) (so-called Sato EoS) were developed by us.[9] A simple mixing rule with binary interaction parameters applied to the EoS is proposed here.

The basic function of the EoS for mixtures is expressed with three temperature-dependent parameters, A_m, C_m,

Table 4. Experimental Liquid Phase *PVTx* Data for the Ternary System Propane (1) + *n*-Butane (2) + Isobutane (3)

T/K	P/kPa	ρ/kg·m^{-3}	T/K	P/kPa	ρ/kg·m^{-3}	T/K	P/kPa	ρ/kg·m^{-3}	T/K	P/kPa	ρ/kg·m^{-3}	T/K	P/kPa	ρ/kg·m^{-3}	T/K	P/kPa	ρ/kg·m^{-3}
			$(x_1, x_2) = (0.200, 0.600)$									$(x_1, x_2) = (0.340, 0.330)$					
240.000	6983.2	628.52	240.000	6523.4	628.06	240.000	6030.7	627.57	300.000	3950.3	547.17	300.000	3482.4	546.23	300.000	3023.2	545.27
240.000	5507.0	627.05	240.000	5013.9	626.56	240.000	4526.1	626.06	300.000	2443.3	544.02	300.000	1952.5	542.95	300.000	1504.5	541.95
240.000	4018.7	625.56	240.000	3535.2	625.05	240.000	3023.1	624.53	300.000	1019.8	540.85	300.000	538.4	539.75	320.000	7000.7	529.19
240.000	2511.9	623.99	240.000	1983.6	623.45	240.000	1509.1	622.96	320.000	6531.1	528.06	320.000	5939.9	526.61	320.000	5435.5	525.35
240.000	1005.8	622.43	240.000	497.3	621.89	260.000	7034.3	608.44	320.000	4926.5	524.04	320.000	4463.0	522.83	320.000	3970.2	521.51
260.000	6514.4	607.85	260.000	6021.4	607.28	260.000	5515.7	606.69	320.000	3499.4	520.22	320.000	2973.2	518.74	320.000	2441.7	517.21
260.000	5034.2	606.11	260.000	4516.2	605.50	260.000	4021.5	604.90	320.000	1972.6	515.82	320.000	1502.5	514.39	320.000	1007.9	512.84
260.000	3511.7	604.29	260.000	3020.3	603.68	260.000	2502.2	603.04	340.000	7080.6	503.22	340.000	6464.2	501.25	340.000	5950.2	499.56
260.000	1994.4	602.41	260.000	1503.4	601.78	260.000	1010.6	601.15	340.000	5450.2	497.86	340.000	4991.2	496.23	340.000	4489.6	494.42
260.000	507.6	600.50	280.000	7006.6	587.83	280.000	6511.5	587.13	340.000	3985.1	492.53	340.000	3432.2	490.38	340.000	3000.1	488.64
280.000	6002.3	586.41	280.000	5517.8	585.71	280.000	5003.6	584.97	340.000	2508.9	486.57	340.000	2007.6	484.38	340.000	1481.6	481.96
280.000	4514.7	584.25	280.000	3980.5	583.46	280.000	3498.1	582.73	360.000	6995.7	473.74	360.000	6510.1	471.55	360.000	6015.5	469.27
280.000	2997.9	581.96	280.000	2481.0	581.17	280.000	1988.8	580.40	360.000	5513.8	466.82	360.000	5013.2	464.24	360.000	4514.2	461.53
280.000	1502.9	579.64	280.000	992.8	578.83	280.000	512.8	578.05	360.000	4025.5	458.72	360.000	3509.0	455.54	360.000	3014.4	452.30
300.000	7057.6	566.21	300.000	6489.7	565.31	300.000	5993.0	564.33	360.000	2513.4	448.73	380.000	7007.4	438.68	380.000	6507.8	435.17
300.000	5509.0	563.50	300.000	5008.6	562.58	300.000	4518.8	561.78	380.000	6025.5	431.52	380.000	5505.9	427.32	380.000	5029.3	423.11
300.000	4020.0	560.84	300.000	3512.7	559.79	300.000	2991.7	558.81	380.000	4498.4	417.88	380.000	4024.3	412.54	380.000	3551.6	406.51
300.000	2507.5	557.84	300.000	2002.8	556.96	300.000	1506.1	555.86	380.000	3042.5	398.57						
300.000	1009.3	554.90	320.000	7009.0	543.27	320.000	6499.8	542.16				$(x_1, x_2) = (0.600, 0.200)$					
320.000	6025.4	541.11	320.000	5529.0	539.99	320.000	5024.5	538.84	240.000	7061.2	604.03	240.000	6514.7	603.43	240.000	5962.3	602.86
320.000	4515.1	537.65	320.000	3993.8	536.40	320.000	3494.8	535.18	240.000	5423.3	602.28	240.000	4979.3	601.73	240.000	4509.3	601.26
320.000	2991.7	533.93	320.000	2505.3	532.69	320.000	1997.7	531.37	240.000	3982.4	600.64	240.000	3519.7	600.08	240.000	2985.5	599.50
320.000	1500.6	530.04	320.000	1003.0	528.68	340.000	7062.3	518.79	240.000	2469.6	598.85	240.000	1989.6	598.34	240.000	1503.3	597.73
340.000	6507.2	517.22	340.000	6005.9	515.77	340.000	5513.6	514.31	240.000	970.0	597.10	240.000	482.9	596.60	240.000	154.1	596.18
340.000	5000.3	512.74	340.000	4511.6	511.21	340.000	3997.4	509.56	260.000	7087.8	582.45	260.000	6455.0	581.62	260.000	5994.9	581.01
340.000	3493.5	507.88	340.000	2977.2	506.10	340.000	2500.3	504.41	260.000	5480.6	580.32	260.000	4938.0	579.60	260.000	4490.3	578.98
340.000	2003.1	502.58	340.000	1509.2	500.72	360.000	7000.9	491.15	260.000	4028.9	578.35	260.000	3469.7	577.57	260.000	2999.4	576.91
360.000	6497.8	489.21	360.000	6014.2	487.29	360.000	5490.1	485.13	260.000	2474.4	576.16	260.000	1985.0	575.46	260.000	1477.1	574.72
360.000	5012.0	483.08	360.000	4503.7	480.80	360.000	3993.4	478.40	260.000	1019.2	574.05	260.000	500.0	573.28	280.000	7065.6	560.33
360.000	3505.4	475.99	360.000	2995.9	473.35	360.000	2503.6	470.65	280.000	6432.5	559.29	280.000	5989.6	558.56	280.000	5474.9	557.71
360.000	2002.9	467.72	380.000	7037.5	459.56	380.000	6474.7	456.31	280.000	5000.1	556.91	280.000	4516.4	556.08	280.000	4018.6	555.22
380.000	5967.1	453.33	380.000	5490.2	450.28	380.000	4978.4	446.88	280.000	3519.6	554.35	280.000	3011.2	553.45	280.000	2491.3	552.51
380.000	4532.8	443.64	380.000	4019.3	439.62	380.000	3514.2	435.32	280.000	2021.0	551.65	280.000	1515.2	550.71	280.000	1001.1	549.74
380.000	3018.0	430.51	380.000	2511.3	425.00				280.000	509.3	548.79	300.000	6988.1	536.64	300.000	6512.1	535.66
			$(x_1, x_2) = (0.340, 0.330)$						300.000	6014.0	534.61	300.000	5491.9	533.49	300.000	5017.8	532.46
240.000	7075.5	617.31	240.000	6492.8	616.70	240.000	5996.3	616.03	300.000	4509.3	531.34	300.000	4012.7	530.21	300.000	3513.5	529.07
240.000	5555.2	615.56	240.000	4961.7	614.94	240.000	4485.4	614.44	300.000	3001.8	527.86	300.000	2511.3	526.69	300.000	1992.9	525.42
240.000	3949.1	613.87	240.000	3481.2	613.35	240.000	3017.6	612.85	300.000	1509.3	524.21	300.000	1004.8	522.92	320.000	6980.1	511.05
240.000	2511.3	612.32	240.000	2001.4	611.77	240.000	1537.4	611.25	320.000	6499.2	509.75	320.000	6017.5	508.43	320.000	5509.4	506.99
240.000	1020.6	610.66	240.000	488.4	610.05	260.000	7019.4	596.73	320.000	4978.4	505.45	320.000	4502.1	504.02	320.000	4019.6	502.54
260.000	6464.9	596.04	260.000	5976.9	595.44	260.000	5496.6	594.86	320.000	3509.9	500.92	320.000	3005.8	499.28	320.000	2509.3	497.61
260.000	4983.9	594.21	260.000	4524.0	593.61	260.000	3996.0	592.94	320.000	1998.1	495.84	320.000	1521.7	494.11	340.000	7017.5	482.83
260.000	3484.6	592.27	260.000	3021.3	591.67	260.000	2526.5	591.01	340.000	6487.2	480.88	340.000	6023.3	479.09	340.000	5508.8	477.01
260.000	1999.3	590.30	260.000	1537.5	589.66	260.000	1002.5	588.93	340.000	5025.7	475.00	340.000	4516.4	472.78	340.000	4004.6	470.46
260.000	497.8	588.25	280.000	6993.6	575.44	280.000	6478.7	574.66	340.000	3467.9	467.89	340.000	2985.2	465.45	340.000	2506.6	462.92
280.000	5967.2	573.88	280.000	5517.7	573.18	280.000	4982.6	572.35	340.000	1972.5	459.90	360.000	6924.7	448.88	360.000	6421.8	445.88
280.000	4481.0	571.55	280.000	4003.6	570.79	280.000	3509.8	569.99	360.000	6007.7	443.33	360.000	4933.6	436.08	360.000	4459.8	432.50
280.000	2986.1	569.13	280.000	2615.2	568.51	280.000	1990.7	567.47	360.000	3925.9	428.10	360.000	3460.8	423.85	360.000	2975.8	418.89
280.000	1513.6	566.66	280.000	1014.3	565.80	280.000	504.1	564.91	380.000	7015.4	409.01	380.000	6484.9	403.74	380.000	6008.8	398.44
300.000	7076.5	553.30	300.000	6514.0	552.24	300.000	5966.4	551.19	380.000	5518.3	392.25	380.000	5010.0	384.67	380.000	4508.9	375.46
300.000	5489.4	550.25	300.000	4947.7	549.19	300.000	4420.2	548.13	380.000	4020.1	363.44						

and D_m, as follows.

$$\rho_{r,m} = \frac{(P_{r,m} + A_m(T_{r,m}))^{C_m(T_{r,m})}}{D_m(T_{r,m})} \tag{5}$$

where $P_{r,m} = P/P_{C,m}$, $T_{r,m} = T/T_{C,m}$ and $\rho_{r,m} = \rho/\rho_{C,m}$ are dimensionless pressure, density, and temperature for the mixture. For a mixture of N components, these critical parameters are expressed as

$$\frac{1}{P_{C,m}} = \sum_i^N \sum_i^N \frac{x_i}{P_{C,i}} \tag{6}$$

$$T_{C,m} = \sum_i^N \sum_j^N x_i x_j T_{C,ij} \tag{7}$$

$$\rho_{C,m} = \sum_i^N \sum_j^N x_i x_j \rho_{C,ij} \tag{8}$$

When $i = j$, $T_{C,ii}$ and $\rho_{C,ii}$ denote the critical temperature and density for component i, respectively. Pseudocritical parameters $T_{C,ij}$ and $\rho_{C,ij}$ $(i \neq j)$ are given by

$$T_{C,ij} = \sqrt{T_{C,ii} T_{C,jj}} \tag{9}$$

$$\rho_{C,ij} = \left[\frac{\rho_{C,ii}^{-1/3} + \rho_{C,jj}^{-1/3}}{2}\right]^{-3} \tag{10}$$

Parameters A_m, C_m, and D_m in eq 5 are given with empirical expressions

$$A_m = \sum_{k=0}^{2} a_{m,k} T_r^k \tag{11}$$

$$C_m = \sum_{k=0}^{2} c_{m,k} T_r^k \tag{12}$$

$$D_m = \sum_{k=0}^{2} d_{m,k} T_r^k \tag{13}$$

We have applied an original mixing rule for these empirical

Table 5. Bubble-Point Pressures and Saturated-Liquid Densities of the Binary and Ternary Systems Composed of Propane (1), *n*-Butane (2), and Isobutane (3)

T/K	P/kPa	ρ/kg·m^{-3}	T/K	P/kPa	ρ/kg·m^{-3}	T/K	P/kPa	ρ/kg·m^{-3}
$(x_1, x_2) = (0.250, 0.750)$			$(x_1, x_2) = (0.500, 0.500)$			$(x_1, x_2) = (0.750, 0.250)$		
			240.000	84.5	606.37	240.000	115.5	589.36
260.000	120.8	600.21	260.000	181.8	584.58	260.000	245.0	566.05
280.000	238.2	577.86	280.000	347.0	560.91	280.000	461.9	541.14
300.000	425.0	554.07	300.000	604.0	535.40	300.000	793.1	514.20
320.000	706.9	528.42	320.000	978.3	507.52	320.000	1270.5	483.71
340.000	1107.1	499.52	340.000	1494.8	475.99	340.000	1928.1	447.59
360.000	1651.1	466.36				360.000	2802.7	398.44
380.000	2372.7	424.79	380.000	3100.2	387.07			
$(x_1, x_2) = (0.250, 0)$			$(x_1, x_2) = (0.499, 0)$			$(x_1, (x_1, x_2) = (0.750, 0)$		
240.000	67.2	607.81				240.000	119.8	583.82
260.000	147.0	585.98	250.000	136.0	584.44	260.000	250.0	560.96
280.000	281.4	562.49	280.000	383.3	549.15	280.000	473.2	535.32
300.000	518.6	537.31	300.000	665.2	522.96	300.000	820.8	507.33
320.000	862.1	509.12	320.000	1077.7	491.75	320.000	1322.1	475.51
340.000	1338.8	478.17	340.000	1641.5	457.03	340.000	2011.3	436.07
360.000	1968.9	440.78	360.000	2403.0	416.83	360.000	2910.6	388.35
380.000	2798.3	390.71	380.000	3362.9	346.90			
$(x_1, x_2) = (0, 0.250)$			$(x_1, x_2) = (0, 0.500)$			$(x_1, x_2) = (0, 0.750)$		
240.000	59.3	621.33	240.000	32.9	625.96	240.000	26.1	630.89
260.000	100.9	600.04	260.000	78.4	604.76	260.000	68.6	609.84
280.000	190.7	577.61	280.000	166.0	582.79	280.000	148.9	588.07
300.000	360.6	553.87	300.000	313.6	559.44	300.000	284.8	564.78
320.000	602.2	527.89	320.000	543.5	534.14	320.000	498.8	540.17
340.000	963.7	499.35	340.000	880.6	506.18	340.000	814.9	512.91
			360.000	1351.0	474.18	360.000	1258.4	481.73
380.000	2136.4	424.73	380.000	1985.6	435.21	380.000	1955.8	445.14
$(x_1, x_2) = (0.200, 0.600)$			$(x_1, x_2) = (0.340, 0.330)$			$(x_1, x_2) = (0.600, 0.200)$		
240.000	52.2	621.44	240.000	71.0	609.76	240.000	101.3	596.11
260.000	116.3	599.87	260.000	153.6	587.73	260.000	214.9	572.86
280.000	231.3	577.64	280.000	299.5	564.58	280.000	406.8	548.59
300.000	415.6	553.78	300.000	527.2	539.77	300.000	703.1	522.16
320.000	694.1	527.78	320.000	864.4	512.41	320.000	1131.6	492.73
340.000	1090.0	499.07	340.000	1336.9	481.32	340.000	1726.2	458.47
360.000	1631.7	465.41	360.000	1976.4	444.57	360.000	2518.4	414.22
380.000	2349.7	423.25	380.000	2810.3	394.93	380.000	3545.7	351.78

Table 6. Numerical Constants for Equations 11−13

substance	propane (1)	*n*-butane (2)	isobutane (3)
ij	11	22	33
T_C/K	369.811	425.125	407.761
P_C/kPa	4248	3796	3631
ρ_C/kg·m^{-3}	222	227.84	233
$a_{ij,0}$	51.528 2	39.031 3	40.081 1
$a_{ij,1}$	−90.297 5	−63.615 8	−66.001 0
$a_{ij,2}$	37.800 7	23.567 2	24.967 5
$c_{ij,0}$	0.102 351	0.072 934	0.077 124
$c_{ij,1}$	−0.077 820	−0.075 024	−0.078 421
$c_{ij,2}$	0.087 578	0.109 702	0.113 271
$d_{ij,0}$	0.404 740	0.352 283	0.369 925
$d_{ij,1}$	0	−0.000 028	−0.000 241
$d_{ij,2}$	0.160 565	0.208 062	0.213 270

constants $a_{m,k}$, $c_{m,k}$, and $d_{m,k}$ that are expressed as follows:

$$a_{m,k} = \sum_{i=1}^{N}\sum_{j=1}^{N} x_i x_j a_{ij,k} \tag{14}$$

$$c_{m,k} = \sum_{i=1}^{N}\sum_{j=1}^{N} x_i x_j c_{ij,k} \tag{15}$$

$$d_{m,k} = \sum_{i=1}^{N}\sum_{j=1}^{N} x_i x_j d_{ij,k} \tag{16}$$

In a similar manner for the critical parameters, a_{ii}, c_{ii}, and d_{ii} are equivalent to the empirical parameters for pure component i. Constants a_0−a_2, c_0−c_2, and d_0−d_2 were determined by an optimum fitting procedure to the experimental data for the pure components and are presented in the literature.[9] Numerical values for these constants are tabulated in Table 1.

Table 7. Statistical Comparison of the Available Mixture Model with the Present Liquid-Phase *PVTx* Data for the Binary and Ternary Systems of Propane (1), *n*-Butane (2), and Isobutane (3)

		propane (1) + *n*-butane (2)		propane (1) + isobutane (3)	*n*-butane (2) + isobutane (3) + propane (1) + *n*-butane (2) + isobutane (3)
LJ model	AAD	0.066	0.153	0.070	0.113
	BIAS	0.039	0.098	0.024	0.087
	STD	0.077	0.165	0.086	0.107
	RMS	0.087	0.192	0.089	0.138
MW model	AAD	0.053	0.123	0.050	0.111
	BIAS	0.036	0.062	0.010	0.097
	STD	0.056	0.151	0.067	0.100
	RMS	0.067	0.163	0.068	0.139
this work	AAD	0.044	0.091	0.022	0.059
	BIAS	-0.019	-0.007	-0.010	0.024
	STD	0.048	0.125	0.027	0.066
	RMS	0.052	0.125	0.029	0.070

When $i \neq j$, a_{ij}, c_{ij}, and d_{ij} denote the cross parameters and are given in terms of k_{ij}, which is the binary interaction parameter.

$$a_{ij,k} = (1 - k_{ij})\sqrt{a_{ii,k}a_{jj,k}} \tag{17}$$

$$c_{ij,k} = (1 - k_{ij})\sqrt{c_{ii,k}c_{jj,k}} \tag{18}$$

$$d_{ij,k} = (1 - k_{ij})\sqrt{d_{ii,k}d_{jj,k}} \tag{19}$$

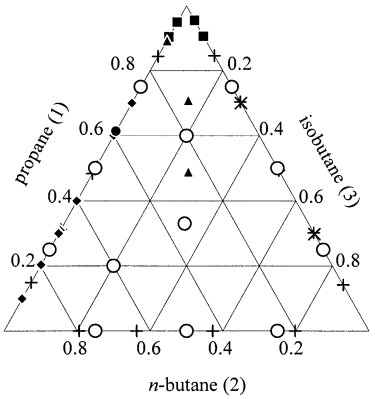

Figure 5. Composition distribution of available *PVTx* data (with numbers of measurements) for the binary and ternary systems of propane (1), *n*-butane (2), and isobutane (3): ○, this work (1167); ×, Duarte-Garza and Magee[16] (341); ●, Holcomb et al.[12] (129); +, Kahre[14] (55); ▲, Luo and Miller[11] (3); ◆, Parrish[13] (513); ■, Thompson and Miller[15] (8).

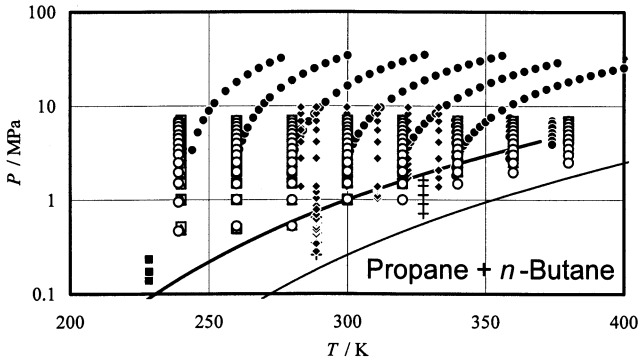

Figure 6. *PVTx* data distribution for the binary system propane (1) + *n*-butane (2), this work: ○, $x_1 = 0.250$; △, $x_1 = 0.500$; □, $x_1 = 0.750$; ●, Holcomb et al.;[12] +, Kahre;[14] ◆, Parrish;[13] ■, Thompson and Miller;[15] calculated vapor-pressure curves, −, propane (1)[1] and −, *n*-butane (2).[2]

Note that when the parameter has a negative value, say, $a_{ii,k}$, $a_{jj,k} < 0$, the parameter for the mixture also becomes negative. Namely,

$$a_{ij,k} = -(1 - k_{ij})\sqrt{a_{ii,k}a_{jj,k}} \qquad (a_{ii,k}, a_{jj,k} < 0) \quad (20)$$

$$c_{ij,k} = -(1 - k_{ij})\sqrt{c_{ii,k}c_{jj,k}} \qquad (c_{ii,k}, c_{jj,k} < 0) \quad (21)$$

$$d_{ij,k} = -(1 - k_{ij})\sqrt{d_{ii,k}d_{jj,k}} \qquad (d_{ii,k}, d_{jj,k} < 0) \quad (22)$$

Binary interaction parameters k_{ij} were determined by fitting the EoS (eq 5) to the liquid-density data for the three binary systems. The parameters thus optimized are given as

$$k_{12} = 0.015150 \quad (23)$$

$$k_{13} = 0.013764 \quad (24)$$

$$k_{23} = -0.00100 \quad (25)$$

No temperature dependence of the interaction parameters was considered.

Comparison with Experimental Data. Relative density deviations of available experimental liquid density data from those calculated by eq 5 are illustrated in Figures 18 to 21.

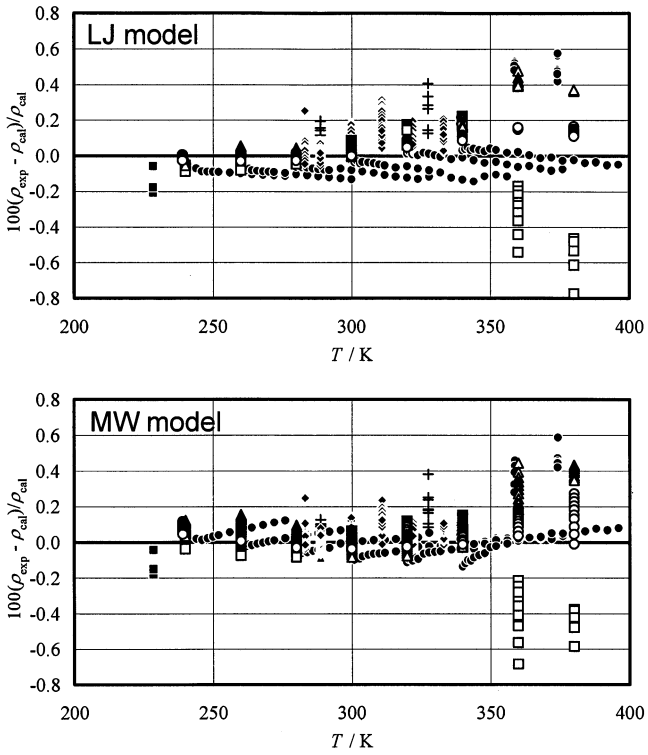

Figure 7. Relative density deviation of the liquid-phase *PVTx* data for the binary system propane (1) + *n*-butane (2) from the Lemmon and Jacobsen model[5] (top) and the Miyamoto and Watanabe model[6] (bottom), this work: ○, $x_1 = 0.250$; △, $x_1 = 0.500$; □, $x_1 = 0.750$; ●, Holcomb et al.;[12] +, Kahre;[14] ◆, Parrish;[13] ■, Thompson and Miller.[15]

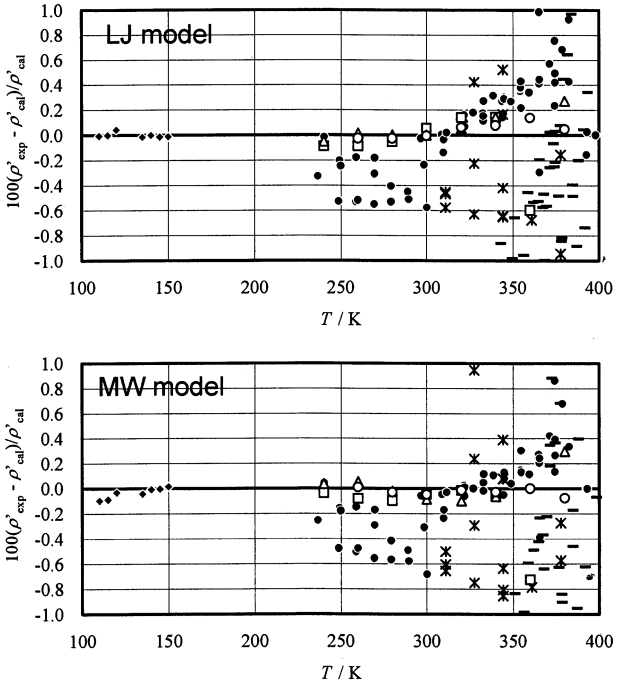

Figure 8. Relative deviation of the saturated-liquid density of the binary system propane (1) + *n*-butane (2) from the Lemmon and Jacobsen model[5] (top) and the Miyamoto and Watanabe model[6] (bottom), this work: ○, $x_1 = 0.250$; △, $x_1 = 0.500$; □, $x_1 = 0.750$; ◆, Hiza et al.,[20] ●, Holcomb et al.;[12] *, Nysewander et al.;[21] −, Kay.[22]

As is seen in Figure 18, the present data for the binary system propane (1) + *n*-butane (2) were excellently represented within ±0.1% at temperatures lower than 340 K.

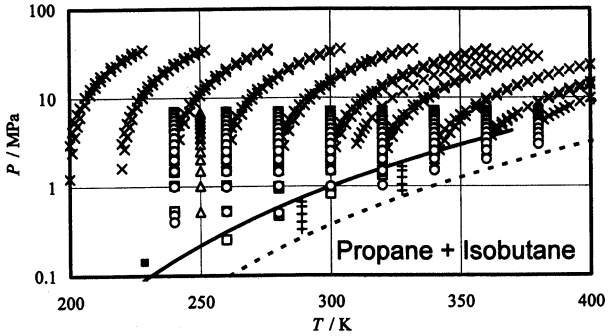

Figure 9. *PVTx* data distribution for the binary system propane (1) + isobutane (3), this work: ○, $x_1 = 0.250$; △, $x_1 = 0.499$; □, $x_1 = 0.750$; ×, Duarte-Garza and Magee;[16] +, Kahre;[14] ■, Thompson et al.;[15] calculated vapor-pressure curves, - -, propane (1)[1] and - - -, isobutane (3).[3]

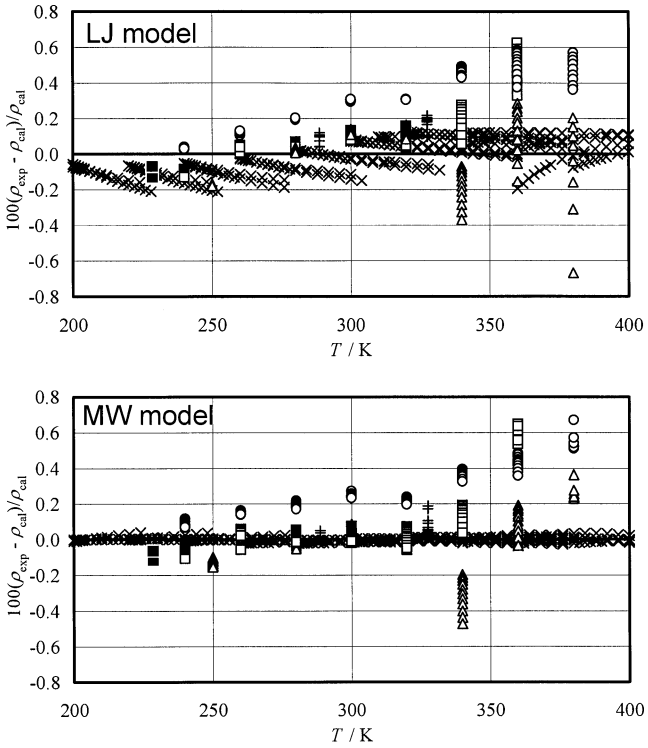

Figure 10. Relative density deviation of the liquid-phase *PVTx* data for the binary system propane (1) + isobutane (3) from the Lemmon and Jacobsen model[5] (top) and the Miyamoto and Watanabe model[6] (bottom), this work: ○, $x_1 = 0.250$; △, $x_1 = 0.499$; □, $x_1 = 0.750$; ×, Duarte-Garza and Magee;[16] +, Kahre;[14] ■, Thompson et al.[15]

In that temperature range, those by Holcomb et al.[12] and Parrish[13] were also reproduced within ±0.2%, whereas those by Kahre[14] deviate by 0.45% at the maximum. Although the pressure range of the data by Holcomb et al. exceeds that of the present work, up to 7 MPa, their data are well represented. However, deviations of the data spread at higher temperatures. They become ±0.5% at 360 K and ±1.0% at 380 K, but these temperatures are higher than the expected temperature limit of the present EoS, being $0.9T_C$.

Similar results were observed in the comparison of the present EoS with the data for the binary system propane (1) + isobutane (3). The scatter of the present data is within ±0.2% where $T \leq 320$ K. It increases to ±0.4% at 340 K and exceeds 1.5% at 380 K. The higher deviations are due to the lower critical temperature of isobutane (3). However, the data by Duarte-Garza and Magee[16] are well repre-

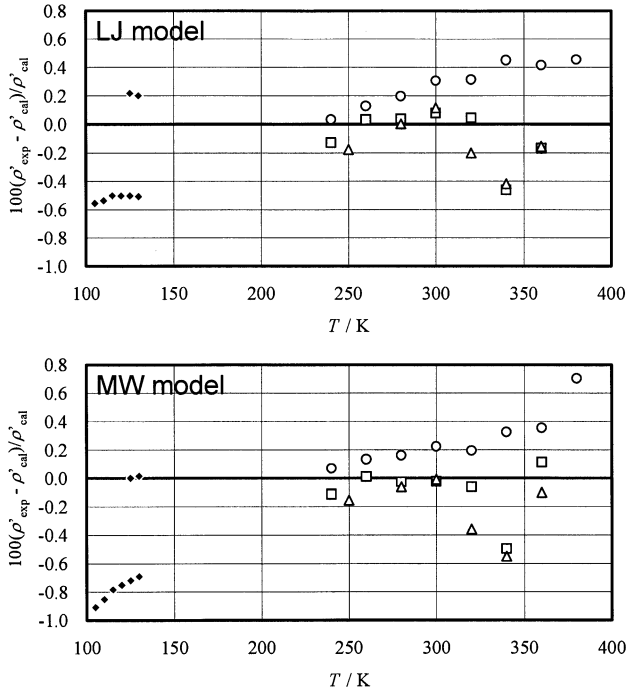

Figure 11. Relative deviation of the saturated-liquid density of the binary system propane (1) + isobutane (3) from the Lemmon and Jacobsen model[5] (top) and the Miyamoto and Watanabe model[6] (bottom), this work: ○, $x_1 = 0.250$; △, $x_1 = 0.499$; □, $x_1 = 0.750$; ◆, Hiza et al.[20]

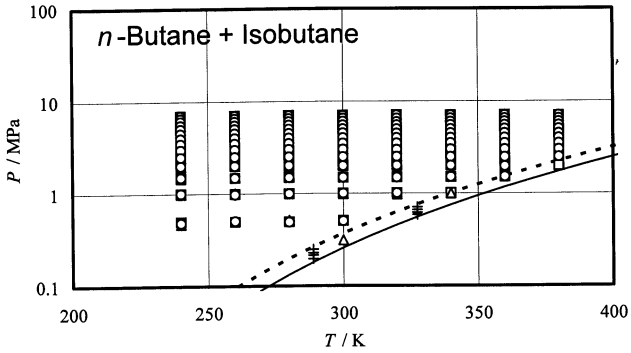

Figure 12. *PVTx* data distribution for the binary system *n*-butane (2) + isobutane (3), this work: △, $x_2 = 0.500$; □, $x_2 = 0.751$; +, Kahre;[14] calculated vapor-pressure curves, - -, *n*-butane (2);[2] - - -, isobutane (3).[3]

sented to within ±0.2% except in the higher temperature range, so the present EoS is expected to have a reporoducibility of ±0.2% within its effective temperature range.

Because the experimental temperature range is lower than the critical temperatures of *n*-butane (2) and isobutane (3), the present EoS can successfully represent the present data for the binary system *n*-butane (2) + isobutane (3) within ±0.1% except at 380 K as shown in Figure 20. The measurements by Kahre[14] also agree with the baseline within ±0.1%.

From Figure 21, the data for the ternary system propane (1) + *n*-butane (2) + isobutane (3) were also well reproduced within ±0.16% except for some data at 380 K for the propane-rich composition (x_1, x_2 = 0.600, 0.200). Because the ternary data could be successfully predicted despite the fact that these data were not used as input data, we can confirm the ability of the present mixing rule. It can be concluded, therefore, that the present EoS can reproduce the liquid-phase *PVTx* properties well over the entire composition range for the ternary system propane

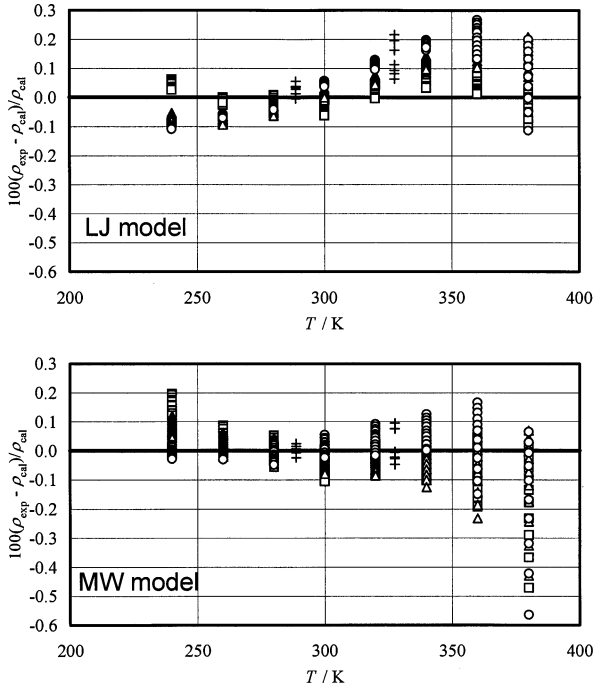

Figure 13. Relative density deviation of the present liquid *PVT* data for the binary system *n*-butane (2) + isobutane (3) from the Lemmon and Jacobsen model[5] (top) and the Miyamoto and Watanabe model[6] (bottom), this work: △, $x_2 = 0.500$; □, $x_2 = 0.751$; +, Kahre.[14]

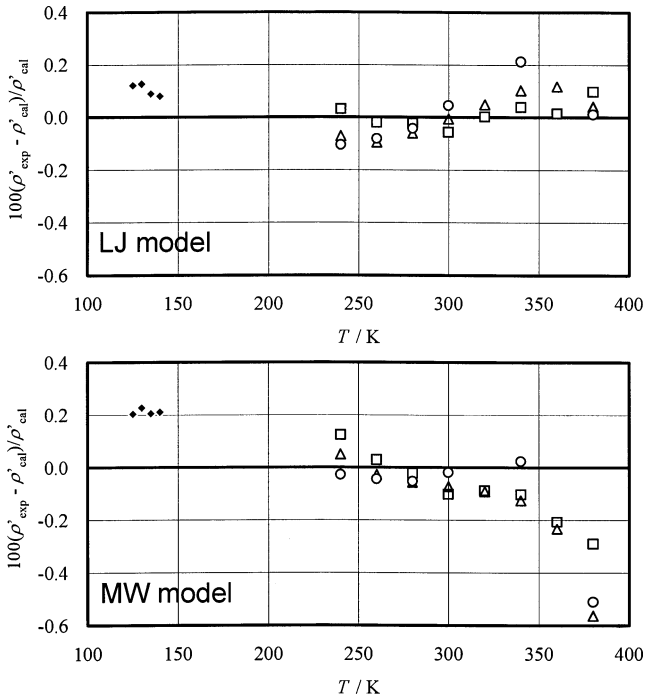

Figure 14. Relative deviation of the saturated-liquid density of the binary system *n*-butane (2) + isobutane (3) from the Lemmon and Jacobsen model[5] (top) and the Miyamoto and Watanabe model[6] (bottom), this work: △, $x_1 = 0.500$; □, $x_1 = 0.751$; *, Hiza et al.[20]

(1) + *n*-butane (2) + isobutane (3), including the binary system and the pure components.

Comparison with the Available Models. The present model for the liquid-phase *PVTx* properties for the binary and ternary systems of propane (1), *n*-butane (2), and isobutane (3) was compared with the available two models of Lemmon and Jacobsen[5] (LJ) and Miyamoto and Watanabe[6] (MW) by calculating the statistical indicators with the present measured data tabulated in Table 2. Only the limited data measured at temperatures lower than $0.9T_C$ were used for the calculation. The definition of the pseudo-critical temperature given in eq 7 was used for the calculation of the reduced temperature.

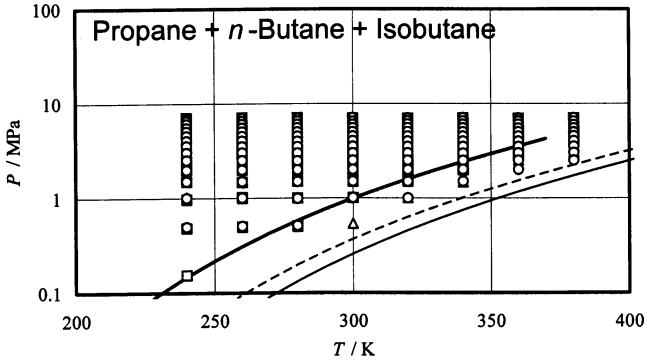

Figure 15. *PVTx* data distribution for the ternary system propane (1) + *n*-butane (2) + isobutane (3), this work: ○, $(x_1, x_2) = (0.200, 0.600)$; △, $(x_1, x_2) = (0.330, 0.340)$; □, $(x_1, x_2) = (0.600, 0.200)$; calculated vapor-pressure curves, −, propane (1),[1] −, *n*-butane (2),[2] and - - -, isobutane (3).[3]

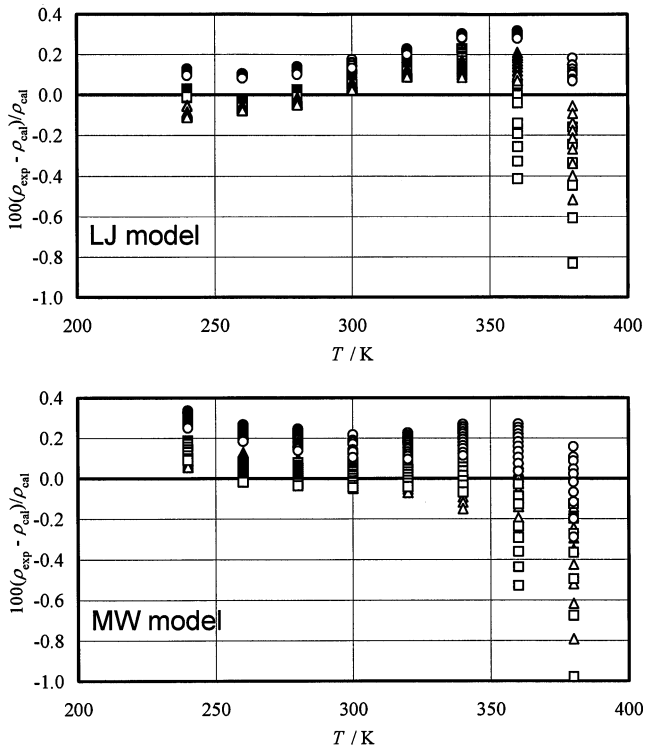

Figure 16. Relative density deviation of the present liquid *PVT* data for the ternary system propane (1) + *n*-butane (2) + isobutane (3) from the Lemmon and Jacobsen model[5] (top) and the Miyamoto and Watanabe model[6] (bottom), this work: ○, $(x_1, x_2) = (0.200, 0.600)$; △, $(x_1, x_2) = (0.330, 0.340)$; □, $(x_1, x_2) = (0.600, 0.200)$.

First, the present model shows the best performance of AAD, BIAS, STD, and RMS because binary interaction parameters k_{12}, k_{13}, and k_{23} were determined from the present data. In the comparison of the other two models, the MW model performs slightly better. Because the LJ model employes the generalized mixing rule that can be applied for any mixture system, the respective reproducibility for a certain mixture is not always better than a model that has been fit to the experimental data. It should also be noted that the LJ model was developed under the condition that the EoS by Younglove and Ely[19] are adopted

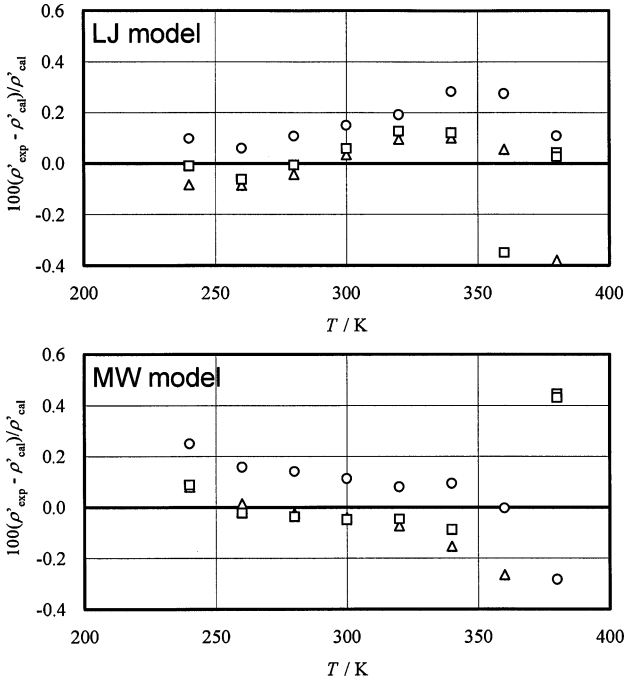

Figure 17. Relative deviation of the saturated-liquid density of the binary system *n*-butane (2) + isobutane (3) from the Lemmon and Jacobsen model[5] (top) and the Miyamoto and Watanabe model[6] (bottom), this work: ○, $(x_1, x_2) = (0.200, 0.600)$; △, $(x_1, x_2) = (0.330, 0.340)$; □, $(x_1, x_2) = (0.600, 0.200)$.

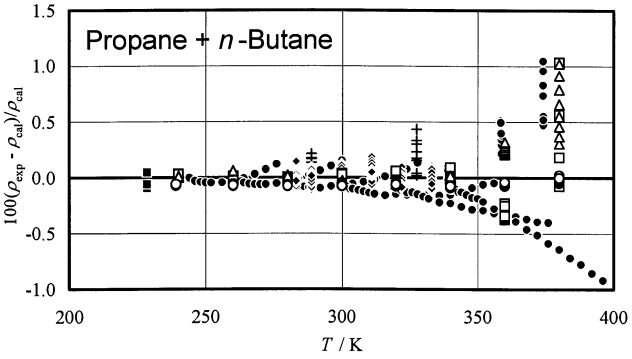

Figure 18. Relative density deviation of the liquid-phase *PVTx* data for the binary system propane (1) + *n*-butane (2) from eq 5, this work: ○, $x_1 = 0.250$; △, $x_1 = 0.500$; □, $x_1 = 0.750$; ●, Holcomb et al.;[12] +, Kahre;[14] ◆, Parrish;[13] ■, Thompson and Miller.[15]

as the part for pure components of propane (1), *n*-butane (2), and isobutane (3). The pure-component part is updated for the EoS by Miyamoto and Watanabe[1,2,3] with the latest version of REFPROP. Hence, it is understood that the LJ model is not optimized with pure-fluid EoS by Miyamoto and Watanabe.

Given such conditions for modeling, the LJ model still shows good performance for the present binary and ternary systems. This is probably because the system consists of similar hydrocarbon components and therefore the thermodynamic behavior of the system is close to the predicted behavior calculated by the generalized mixing rule.

Derived Properties. Subsequently, the consistency of the EoS developed in the present study was examined by calculating the derived properties including the isothermal compressibility κ_T, isobaric heat capacity c_P, and speed of sound w. As examples, these properties for the ternary system with the mole fraction $(x_1, x_2) = (0.6, 0.2)$ were calculated and illustrated in Figures 22 through 24. It

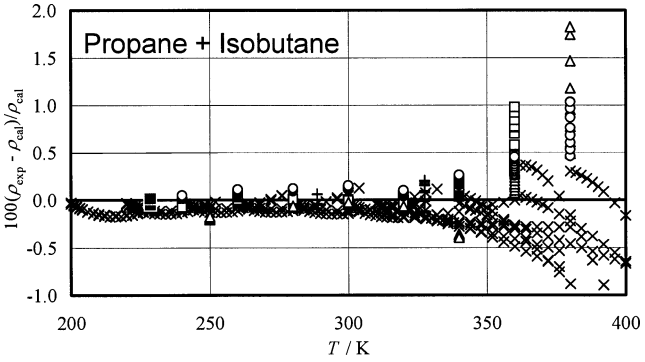

Figure 19. Relative density deviation of the liquid-phase *PVTx* data for the binary system propane (1) + *n*-butane (2) from eq 5, this work: ○, $x_1 = 0.250$; △, $x_1 = 0.499$; □, $x_1 = 0.750$; ×, Duarte-Garza and Magee;[16] +, Kahre;[14] ■, Thompson et al.[15]

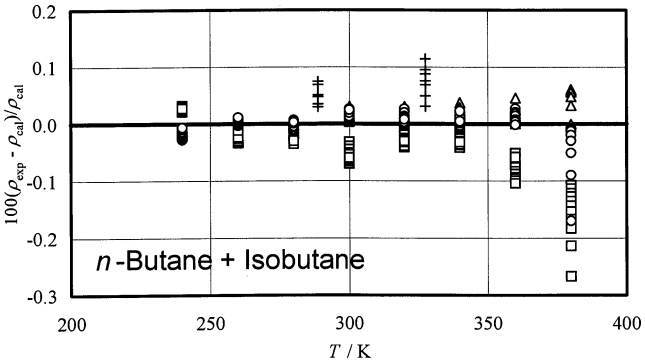

Figure 20. Relative density deviation of the liquid-phase *PVTx* data for the binary system propane (1) + *n*-butane (2) from eq 5, this work: △, $x_2 = 0.500$; □, $x_2 = 0.751$; +, Kahre.[14]

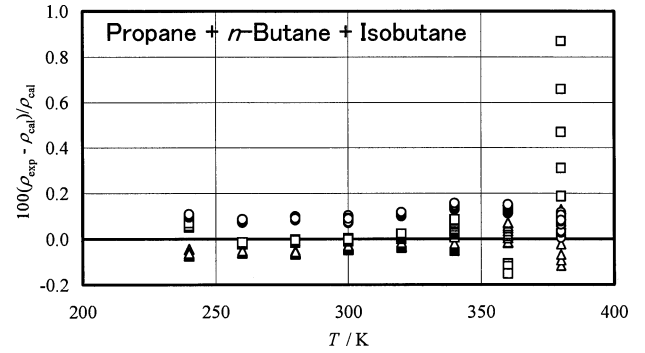

Figure 21. Relative density deviation of the liquid-phase *PVTx* data for the binary system propane (1) + *n*-butane (2) from eq 5, this work: ○, $(x_1, x_2) = (0.200, 0.600)$; △, $(x_1, x_2) = (0.330, 0.340)$; □, $(x_1, x_2) = (0.600, 0.200)$.

should be noted that the isobaric heat capacities for the saturated liquid were calculated from the MW model.[6]

$$c_P = c_P' - \int_{P_S}^{P} T\left(\frac{\partial^2 v}{\partial T^2}\right)_P \mathrm{d}P \tag{26}$$

$$w = \sqrt{\frac{c_P}{\rho \alpha_T c_v}} \tag{27}$$

$$\kappa_T = \frac{C}{A + P} \tag{28}$$

As for the EoS for the pure components, reasonable behavior of the property surface was confirmed.[9] However, the present mixing rule is applied for each of the numerical

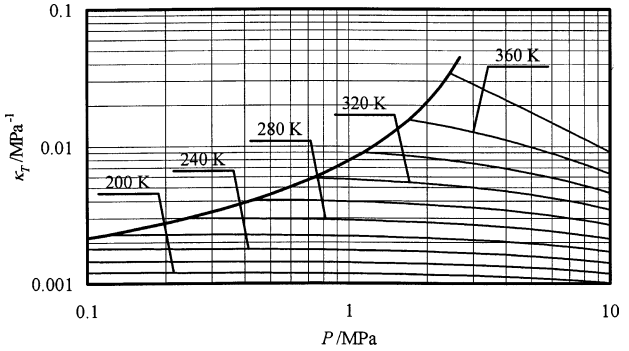

Figure 22. Pressure dependence of the isothermal compressibility for the ternary system propane (1) + *n*-butane (2) + isobutane (3) (x_1, x_2) = (0.6, 0.2) derived from eq 5.

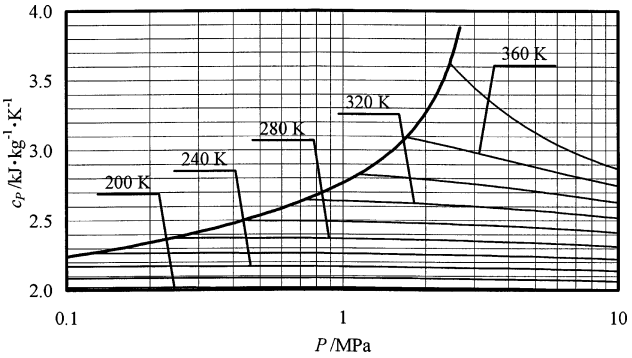

Figure 23. Pressure dependence of the isobaric heat capacity for the ternary system propane (1) + *n*-butane (2) + isobutane (3) (x_1, x_2) = (0.6, 0.2) derived from eq 5.

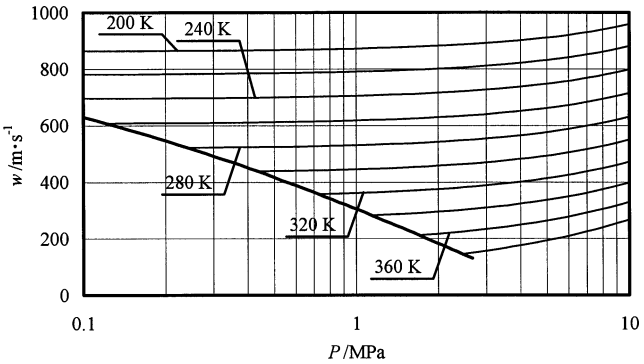

Figure 24. Pressure dependence of the speed of sound for the ternary system propane (1) + *n*-butane (2) + isobutane (3) (x_1, x_2) = (0.6, 0.2) derived from eq 5.

constants $a_{m,0}$ through $d_{m,2}$, so it does not necessarily mean that the calculated mixture properties are thermodynamically compatible. Figures 22 through 24 show that thermodynamically sound behavior of these derived properties are clearly observed. Therefore, it can be concluded that the present mixing rule not only satisfactory reproduces the *PVTx* properties over the entire composition range but that it is also thermodynamically consistent.

Conclusions

In the present study, more than 1000 *PVTx* properties were obtained for the binary and ternary systems of propane (1), *n*-butane (2), and isobutane (3). The bubble-point pressures and saturated-liquid densities were also reported. The present measurements contain the first set of *PVTx* properties for the ternary system and also the first wide-range data for the binary system *n*-butane (2) + isobutane (3).

The measured data were compared with two available mixture thermodynamic models, the Lemmon and Jacobsen model[5] and the Miyamoto and Watanabe model.[6] As a result of the comparison, it was found that both models represent the present data well within ±0.2% at moderate temperatures ($T < 0.9T_C$) but the deviation spreads at higher temperatures.

On the basis of the present measurements, a simple mixing rule for the modified Tait equation of state (Sato EoS) that was fitted separately to the pure-component data was proposed. By employing binary interaction parameters k_{ij}, not only the binary *PVTx* properties but also the ternary data were well reproduced. The themodynamically sound behavior of the EoS was also confirmed by calculating the property surfaces of the isothermal compressibility, isobaric heat capacity, and speed of sound.

Acknowledgment

We are grateful to Dr. Hiroyuki Miyamoto for the calculations with his EoS program and for offering the literature data.

Literature Cited

(1) Miyamoto, H.; Watanabe, K. A Thermodynamic Property Model for Fluid-Phase Propane. *Int. J. Thermophys.* **2000**, *21*, 1045−1072.
(2) Miyamoto, H.; Watanabe, K. A Thermodynamic Property Model for Fluid-Phase *n*-Butane. *Int. J. Thermophys.* **2001**, *22*, 459−475.
(3) Miyamoto, H.; Watanabe, K. A Thermodynamic Property Model for Fluid-Phase Isobutane. *Int. J. Thermophys.* **2002**, *23*, 477−499.
(4) Lemmon, E. W.; McLlinden, M. O.; Huber, M. L. *REFPROP, Reference Fluid Thermodynamic and Transport Properties*; NIST Standard Reference Database 23, version 7.0.; National Institute of Standards and Technology, U.S. Department Commerce: Washington, DC, 2002.
(5) Lemmon, E. W.; Jacobsen, R. T. A Generalized Model for the Thermodynamic Properties of Mixtures. *Int. J. Thermophys.* **1999**, *20*, 825−835.
(6) Miyamoto, H.; Watanabe, K. Helmholtz-type Equations of State for Hydrocarbon Refrigerant Mixtures of Propane/*n*-Butane, Propane/Isobutane, *n*-Butane/Isobutane, and Propane/*n*-Butane/Isobutane. *Int. J. Thermophys.* **2003**, *24*, 1007−1031.
(7) Kayukawa, Y.; Hasumoto, M.; Watanabe, K. Rapid Density-Measurement System with Vibrating Tube Densimeter. *Rev. Sci. Instrum.* **2003**, *74*, 4134−4139.
(8) Kayukawa, Y.; Hasumoto, M.; Kano, Y.; Watanabe, K. Thermodynamic Property Measurements for Trifluoromethyl Methyl Ether and Pentafluoroethyl Methyl Ether. *J. Chem. Eng. Data*. **2003**, *48*, 1141−1151.
(9) Kayukawa, Y.; Hasumoto, M.; Kano, Y.; Watanabe, K. Liquid-Phase Thermodynamic Properties for Propane (1), *n*-Butane (2), and Isobutane (3). *J. Chem. Eng. Data*. **2005**. This issue.
(10) Kayukawa, Y. A Study of Thermodynamic Properties for Novel Refrigerants with Rapid and Precise Density Measurement Technique. Ph.D. Thesis, Keio University, Yokohama, Japan, 2002.
(11) Luo, C. C.; Miller, R. C. Densities and Dielectric Constants for Some LPG Components and Mixtures at Cryogenic and Standard Temperatures. *Cryogenics* **1981**, *21*, 85−93.
(12) Holcomb, C. D.; Magee, J. W.; Haynes, W. M. *Density Measurements on Natural Gas Liquids*; Technical Report PR-147; Gas Processors Association: Tulsa, OK, 1995.
(13) Parrish, W. R. Compressed Liquid Densities of Propane - Normal Butane Mixtures between 10 and 60 °C at Pressures up to 9.6 MPa. *Fluid Phase Equilib.* **1986**, *25*, 65−90.
(14) Kahre, L. C. Liquid Density of Light Hydrocarbon Mixtures. *J. Chem. Eng. Data*. **1973**, *18*, 267−270.
(15) Thompson, R. T., Jr.; Miller, R. C. Densities and Dielectric Constants of LPG Components and Mixtures at Cryogenic Storage Conditions. *Adv. Cryog. Eng.* **1980**, *25*, 698−708.
(16) Duarte-Garza, H. A.; Magee, J. W. Isochoric $p-\rho-T$ and Heat Capacity C_v Measurements on $\{xC_3H_8 + (1 - x)i\text{-}C_4H_{10}$, $x \approx 0.7$, 0.3$\}$ from 200 to 400 K at Pressures to 35 MPa. *J. Chem. Eng. Data*. **1999**, *44*, 1048−1054.
(17) Haynes, W. M.; Goodwin, R. D. *Thermophysical Properties of Normal Butane from 135 to 700 K at Pressures to 70 MPa*; NBS Monograph 169; National Bureau of Standards: Washington, DC, 1982.

(18) Yoshii, Y. Measurements of Saturation Densities and Critical Parameters for Alternative Refrigerants with Less Environmental Impact (in Japanese). Master's Thesis, Keio University, Yokohama, Japan, 2001.
(19) Younglove, B. A.; Ely, J. F. Thermophysical Properties of Fluids. II. Methane, Ethane, Propane, Isobutane and Normal Butane. *J. Phys. Chem. Ref. Data*. **1987**, *16*, 577−798.
(20) Hiza, M. J.; Haynes, W. M.; Parrish, W. R. Orthobaric Liquid Densities and Excess Volumes for Binary Mixtures of Low Molar Mass Alkanes and Nitrogen between 105 and 140 K. *J. Chem. Thermodyn*. **1977**, *9*, 873−896.
(21) Nysewander, C. N.; Sage, B. H.; Lacey, W. N. Phase Equilibria in Hydrocarbon Systems. The Propane−*n*-Butane System in the Critical Region. *Ind. Eng. Chem.* **1940**, *32*, 118−123.
(22) Kay, W. B. Vapor−Liquid Equilibrium Relations of Binary Systems. The Propane−*n*-Alkane Systems. *n*-Butane and *n*-Pentane. *J. Chem. Eng. Data.* **1970**, *15*, 46−53.

Received for review September 14, 2004. Accepted November 10, 2004. Financial support by the Grant-in-aid for Scientific Research Fund from 2000 to 2002 (project no. 12450090), Ministry of Education, Culture, Sports, Science and Technology, Japan, is acknowledged.

JE049671T